DIPARTIMENTO DI SCIENZE BIOMOLECOLARI

CORSO DI DOTTORATO DI RICERCA
IN SCIENZE DELLA VITA, SALUTE E BIOTECNOLOGIE

Curriculum Biologia della Cellula e della Salute

CICLO XXXI

Starvation-dependent differential stress resistance: a new frontier for radiotherapy?

SSD:BIO/16

RELATORE

Chiar.mo Prof. Loris Zamai

DOTTORANDA

Dott.ssa Sara Pignatta

ANNO ACCADEMICO 2017/2018

Index

Abstract

Since its discovery in the 19th century, radiotherapy has been one of the major medical treatments in oncology, providing curative, adjuvant and palliative therapy and improving overall survival. However, a low dose of irradiation (IR) is delivered outside the tumor target volume, increasing side effects and modifying the interaction between cancer and surrounding stromal cells. Recently, the role of fasting or short term starvation (STS) for cancer patients receiving chemotherapy has been taken into account to enhance therapeutic index and to prevent side effects, but no data are available from patients receiving radiotherapy. Here we investigated *in vitro* the effect of STS on the efficacy of radiotherapy in tumor cell lines derived from primary and metastatic site, and in normal cell lines.

Cells were incubated in low glucose (0.5gr/l + 1%FBS) (STS condition) or normal glucose (1gr/l + 10 %FBS) DMEM medium for 24 hours and treated with a single dose of 5Gyx1 (normal fibroblasts and adenocarcinoma cells), 10Gyx1 (metastatic prostate cell line) and 8Gyx1 (metastatic pancreatic cell line). For the irradiation experiments, the flasks containing the cells were placed in a plexiglass custom-built phantom developed to mimic the passage of radiation through human tissue. The levels of DNA damage were evaluated using alkaline comet assay.

The results indicated that after STS the radiation dose significantly increased levels of DNA damage in metastatic cancer cell lines but not in normal cells, compared to baseline values. Furthermore, using clonogenic assay, we observed that STS had a significative radiosensitizing effect on metastatic cell lines, reducing significantly the surviving fraction. Conversely, such radiosensitizing effect was not observed in fibroblastic cells. Moreover, our *in vitro* results indicate that adenocarcinoma patients could not take advantage of short-term starvation before radiotherapy.

In conclusion, our results suggest that changings in cancer metabolism due to starvation could enhance the efficacy of radiotherapy treatment in *in vitro* metastatic cancer cells without impact on survival fraction of healthy cells.

Poster session: Starvation-induced metabolic changing: a boost for radiotherapy treatment in cancer?

Sara Pignatta, Loris Zamai, Chiara Arienti, Claudia Cocchi, Michele Zanoni, Michela Cortesi, Anna Sarnelli, Donatella Arpa, Filippo Piccinini, Anna Tesei.

EACR: Mechanisms to Therapies: Innovations in Cancer Metabolism, Bilbao, 2018

1. Introduction

1.1. General principles of Radiotherapy

Radiotherapy (RT) is one of the major medical treatments in oncology, providing curative, adjuvant and palliative treatments and improving overall survival.

At present, numerous efforts in four main fields such as delivery and dose prescription, dose distribution and new technology, integration of image-guidance, and radiobiological studies are being devoted to improving radiotherapy. Radiobiology aims to study and clarify the molecular and cellular responses to radiation-induced damage that influence cell death. In particular, the effects of radiation exposure on biological systems are divided into three phases, physical, chemical and biological (Joiner, 2009).

The physical phase is characterized by ionization and excitation of atoms and molecules ionization. Then, in the chemical phase, the absorbed energy is converted in thermodynamic energy transfer, producing reactive compounds and free radicals. In the biological phase, the action of ionizing radiation produces direct or indirect damage to the main targets: the nuclear DNA (nDNA), mitochondria and mitochondrial DNA (mtDNA), cytoplasm and cell membrane. The nDNA and mtDNA damage, as DNA single-strand break (SSB) or DNA double-strand break (DBSs) can arrest cell proliferation or induce apoptosis *in vitro* and inhibit tumor growth *in vivo*.

However, the efficacy of radiotherapy is limited by its toxicity, because a low dose of irradiation (IR) is delivered outside the tumor target volume, increasing side effects (*e.g.* myelosuppression, cognitive dysfunction, and esophagitis) and modifying the interaction between cancer and surrounding stromal cells.

Over time, the radiation dose fractionation has been one of the most successful strategies to reduce side-effects , due to its capacity to perturb the four major parameters of radiation response **(**Withers et al., 1999):

1. Repair of the sublethal damage: exposure of biological tissues to ionizing radiation leads to DNA damage. The repair DNA system could repair DNA lesions if a time delay is allowed before the second ionization dose. If the distance between the two doses is reduced, a minor radiation dose fraction will be necessary to induce the same tissue damage.
2. Hypoxic cell re-oxygenation: hypoxic cells are less sensitive to ionizing radiation than oxygenated cells. A change in the tumor hypoxic fraction occurs during fractionated radiotherapy, due to the death and elimination of well oxygenated tumor cells with consequent tumor re-oxygenation.

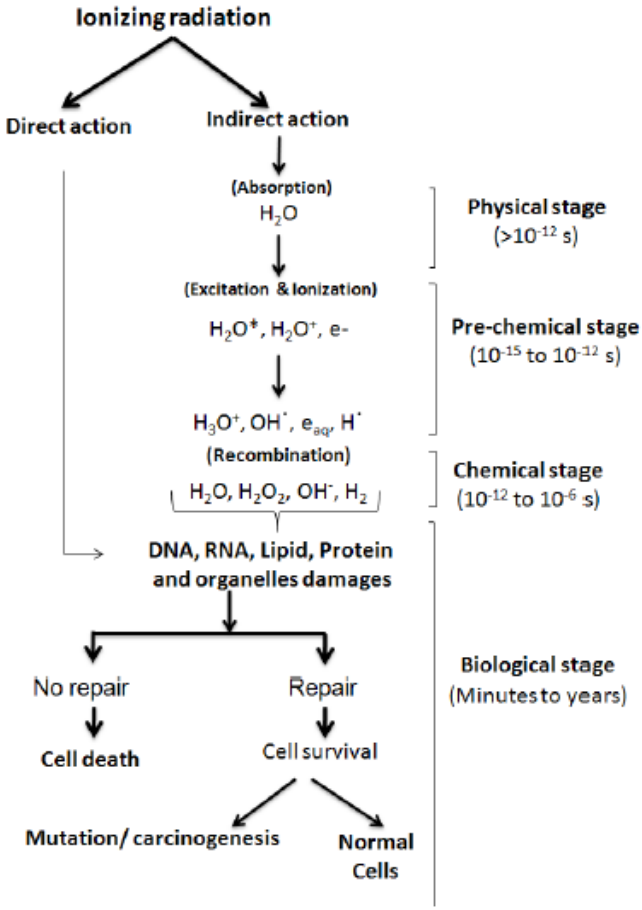

Figure 1: Time-scale of radiation effects on the biological system (Maurya et al., 2011).

3. Cell cycle redistribution: The related cell cycle phases have a different radiosensitivity: cells in late G2 and M phase are the most sensitive together with the initial part of G1, while cells in the S phase are the most resistant. In practice, this entails a preferential killing of sensitive cells and a consequent semi-synchronization of the residual population in resistant phases. However, de-synchronization of surviving cells takes place between radiation dose fractions, determining a new radiosensitization.

4. Tissue Repopulation: in response to the depopulation determined by irradiation, both healthy and tumor tissues increase proliferative activity. This phenomenon translates into the need for an increase in the total radiation dose to obtain the same effect.

Any strategy that selectively increases the radiosensitivity of tumor cells and radioresistence in normal cells is an appreciable factor to add to RT.

The identification of potentially metabolic mechanisms that underlie the response of tumor and normal tissue to irradiation could contribute to new treatment strategies and drive to specific clinical protocols.

1.2. Cell Cycle

The radiosensitivity of cells depends as they pass through the cell cycle. A cell's life is divided into the following phases:

- phase G1: an increase in the biosynthetic activities is determined to prepare the cell for the duplication of the different cellular components,
- S phase: begins with DNA synthesis and ends when all the chromosomes have been duplicated
- phase G2: temporal period between the phases S and M
- phase M: mitosis proceeds as a continuous sequence of events divided into five stages: prophase, prometaphase, metaphase, anaphase, tele-phase; it also includes cytokinesis.

All movement through the cycle phases is regulated by a group of serine-threonine kinases called cyclin-dependent kinases (CDKs). Their enzymatic function is active when they are linked with regulatory subunits called cyclin. The several cyclin-CDK complexes are involved at a different cell cycle steps, determining the activation of specific functions related to cell proliferation.

The ordered progression of the phases of the cell cycle is guaranteed by control points ("check-points") that inhibit the transition to a subsequent phase of the cell cycle if the previous phase has not been completed correctly (Foster et al., 2010).

Checkpoints take place at the late stage G1 (checkpoint G1), between the transition from G2 phase and S phase (checkpoint G2), and within mitosis between metaphase and anaphase transition.

CDKs activity influences the checkpoint activation and guarantees a crosstalk between cell cycle arrest and DNA damage response machine.

	G1	S	G2–M
DSBs or single-strand breaks	NHEJ	HR-mediated fork restart	HR-mediated repair
Mismatches		Mismatch repair	
Bulky lesions	NER	Template-switch-mediated damage bypass	
		TLS-mediated damage bypass	

Table 1: Crosstalk between cell cycle checkpoints and DNA-repair events (Branzei et al., 2008).

The modification of molecular pathways (such as diet intervention) that coordinate the signals between these two complex cellular processes might be used to induce a temporary cell-cycle arrest, to preserve genome integrity or to implement the radiation therapy efficacy.

1.3. The DNA damage response

Maintaining genetic stability is essential for organism survival. Therefore, a specialized repair system is developed by cells and organisms to protect DNA from several endogenous and exogenous agents (*e.g.* chemicals, UV, ionizing radiation). The DNA repair machinery is composed by several processes and the choice of which system to use depends on the type of DNA lesions and on the cell-cycle phase (Branzei et al., 2008).

The efficient DNA repair is dependent by precise control points in which coordinated DNA damage sensors proteins and effector proteins allow repair and prevent the genetic lesions transmission to cell progeny. Since DNA is an extremely reactive molecule, numerous mechanisms are evolved by the eukaryotic cell to repair different type of DNA lesions. The main repair mechanisms are described below.

The double-strand breaks (DSBs), the most destructive damages to DNA, are repaired through two mechanisms, non-homologous end joining (NHEJ) or homologous recombination repair (HR). NHEJ is activated during the G1 phase in which a second genome copy is not yet available. Therefore the enzyme DNA ligase IV uses overhanging pieces of DNA adjacent to the break, to join and fill in the ends. Additional errors can be introduced during this process, such as a loss of genetic information or translocation. In contrast, during HR, the homologous chromosome is used as a template to repair damaged DNA. HR is predominantly active during phase S and G2, involving many factors including RAD proteins with recombinase activity and BRCA1 and BRCA2 proteins.

On the other hand, base excision repair (BER) and nucleotide excision repair (NER) are the machineries involved in DNA damage which arises during normal cellular metabolism.
In particular, BER is the predominant mechanism that handles the spontaneous DNA damage caused by free radicals and other reactive species generated by metabolism; while nucleotide excision repair NER repairs lesions produced by exogenous mutagenic agents that cause DNA double helix distortion (*e.g.* pyrimidine dimers produced by UV radiation and Cisplatin-induced complexes). A large multi-enzymatic complex performs a DNA scan looking for a distortion in the double helix rather than a specific change of a base; when the lesion is detected, a DNA-helicase excise the section of damaged DNA and DNA polymerase and DNA ligase filling the gap and seal the nick between the newly synthesized and older DNA.

Furthermore, during DNA synthesis, the base-base mismatches and small insertion or deletion loops are repaired by mismatch repair (MMR). MMR is a post-replication repair system that recognizes and corrects the erroneous sequences in the brother filament. The main genes involved in this mechanism are: hMLH1, hMSH2, hMSH3, hMSH6.

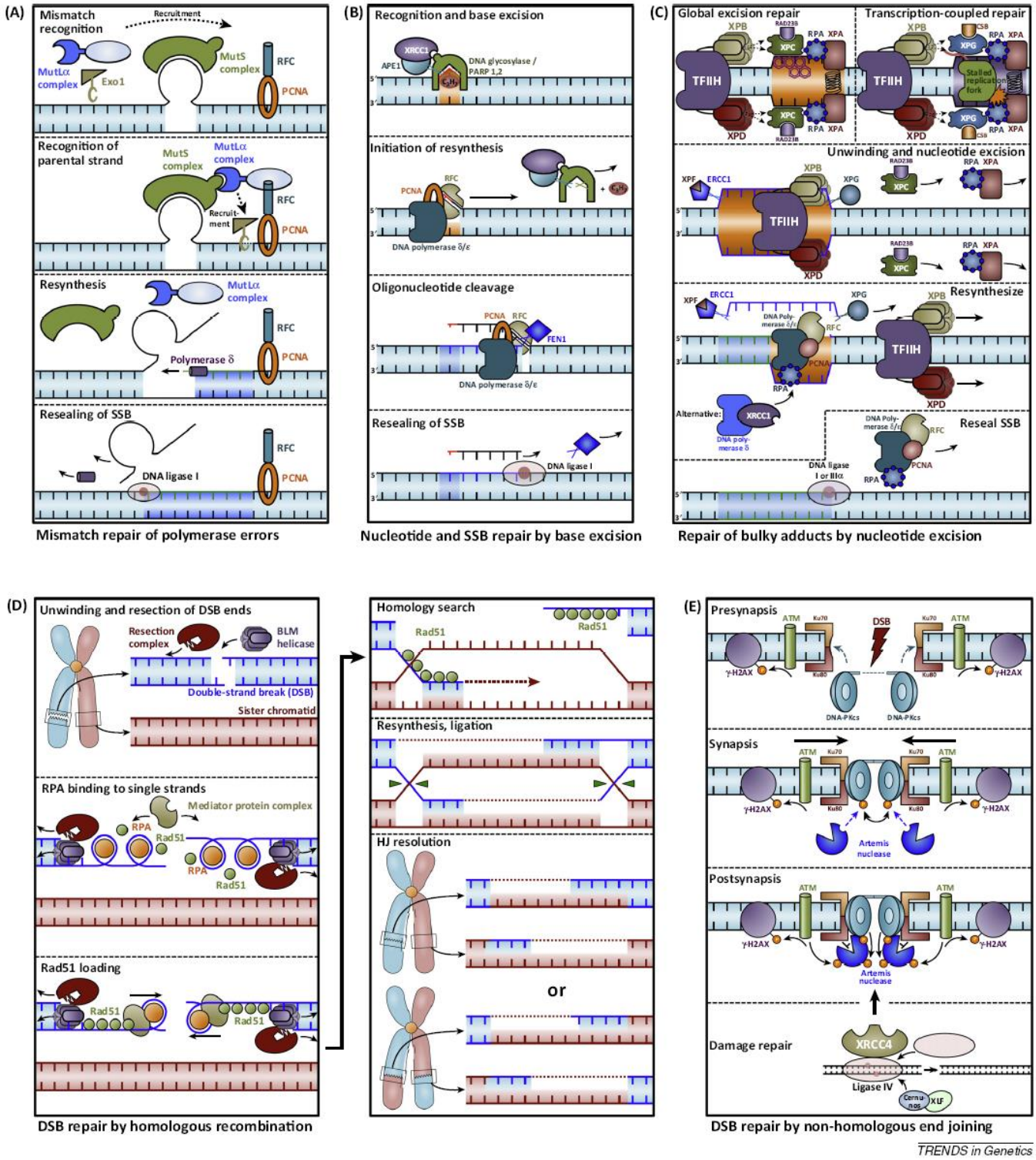

Figure 2: Overview of DNA damage repair pathway (Dietleine et al., 2014)

An important function for an efficient DNA repair is carried out by cell cycle checkpoints. The activation of cell cycle checkpoints mediates cell-cycle arrest and provides time to repair and recover from DNA lesions.

In the field of oncology, this has led to the development of checkpoint inhibitors that do not directly induce DNA breaks but are used as adjuvants to DNA damaging agents, improving their therapeutic effects (Javle et al., 2011; Morales et al., 2014).

Consequently, the cell cycle starvation resulting from caloric restriction or fasting could be a hopeful adjuvant for radiotherapy treatment. Some studies report in animal models improvement in overall survival with the combination of caloric restriction diets and radiotherapy.

These results and further research in this field could have important implications for the design of radiotherapy clinical trials and for understanding the mechanism underlying the association of metabolism and DNA repair machinery.

1.4. Physiological metabolic change due to starvation.

Metabolism is a combination of anabolic and catabolic biochemical reactions that occur within cells, leading to proliferation, support and maintenance processes. In the course of remarkable progress in cancer research, new observations have considered to clarify the biochemical bases of some hallmarks of cancer including sustaining proliferation signaling, evading growth suppressors and resisting cell death. Recently, the role of diet for cancer patients receiving chemotherapy is becoming a new approach to enhancing therapeutic index and to prevent side treatment effects (American Institute for Cancer Research).

Dietary changes can affect tumor growth modifying the blood concentrations of many biomolecules and metabolites. Currently, several dietary interventions are under clinical investigations, including short-term starvation, ketogenic diets, and fasting-mimicking diet.

The post-absorptive state after a meal (fed state), in which glucose and amino acids are transported from intestine to the blood, is characterized by insulin secretion by B cells of pancreas, storage of glucose in glycogen by liver, entry of glucose into muscle and adipose tissue providing synthesis of triacylglycerols and proteins (Berg et al., 2002).

The starvation condition is divided into an early and late fasting state; the first one is characterized by insulin drop and glucagon secretion by pancreatic alpha cells, because the blood-glucose level must be maintained above 2.2.mM (40 mg/dl). Glucagon induces a mobilization, a breakdown of

glycogen (hydrolysis of glucose 6-phosphate) and its release by liver to blood, in order to provide glucose fuel for brain and other tissue.

At the beginning of the early phase, carbohydrate stores are the main component of body fuel, thereafter, the unique sources are fat and proteins. After about 3 days, the majority of energy needs is supplied by ketone bodies, because the second priority of metabolism during starvation is to preserve protein from breakdown into amino acids (Lignot).

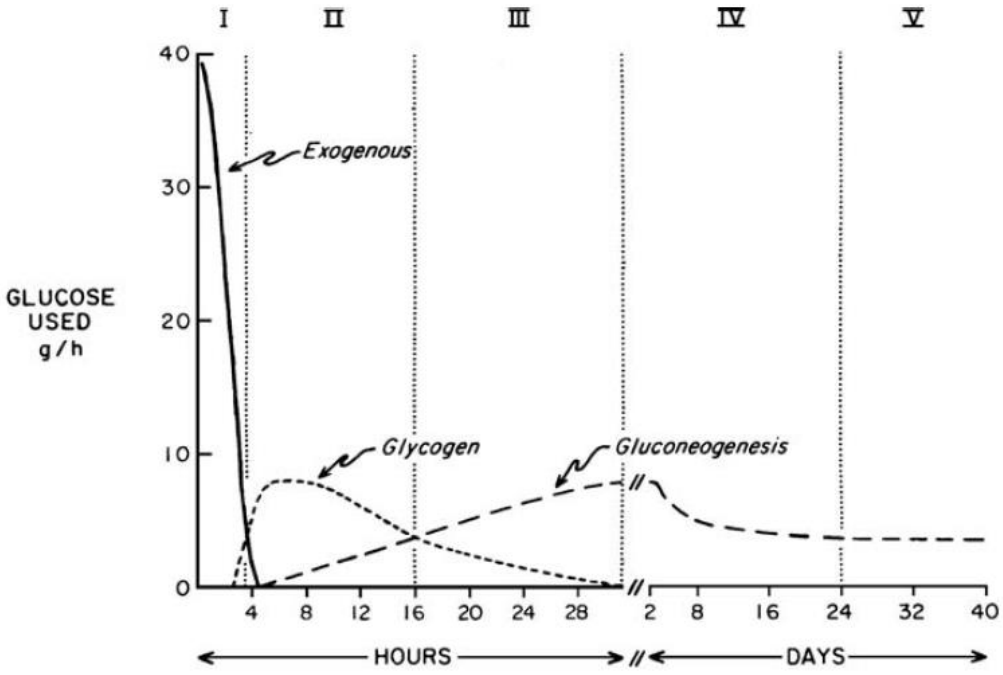

		(I)	(II)	(III)	(IV)	(V)
ORIGIN OF BLOOD GLUCOSE	:	Exogenous	Glycogen Hepatic gluco-neogenesis	Hepatic gluconeo-genesis Glycogen	Gluconeogenesis, hepatic and renal	Gluconeogenesis, hepatic and renal
TISSUES USING GLUCOSE	:	All	All except liver. Muscle and adipose tissue at diminished rates	All except liver. Muscle and adipose tissue at rates intermediate between II and IV	Brain, rbcs, renal medulla. Small amount by muscle	Brain at a diminished rate, rbcs, renal medulla
MAJOR FUEL OF BRAIN	:	Glucose	Glucose	Glucose	Glucose, ketone bodies	Ketone bodies, glucose

Figure 3: The metabolic changes between the post-absorptive and prolonged starvation (Cahill, 2006).

After the depletion of the triacylglycerol stores, the only option is protein degradation, resulting in a dramatic body mass loss, accompanied by heart, liver and kidney loss functions.

Mobeus *et al.* measured blood glucose after a caloric restriction and determined that to maintain glucose homeostasis, the human body adjusts glucose levels after 3 h.

Some animal experiments (Jensen et al., 2013) demonstrated that initiating fasting at different points of the circadian rhythm could have different impacts on physiological parameters such

us, hormone balance, hepatic enzymes and toxicological responses, due to the high nocturnal metabolic rate of mice. Because of these observations, we decided to apply a 24 hours short-term restriction. This allowed us to standardize the experiments and get closer to a potential clinical application in patients.

1.5. Tumor cell metabolism and radiotherapy

Cancer is the second leading cause of mortality counting 8.9 million deaths in 2016 (healthdata.org). As well note, carcinogenesis is a multifactorial process characterized by mutations in oncogenes and tumor suppressor genes responsible for cancer proliferation and metabolic pathway dysregulation. One of the emerging hallmarks of cancer is metabolic dysregulation. As described by Warburg in 1924, the cancer metabolic change is associated with high glucose uptake, with upregulation of glycolysis and downregulation of oxidative phosphorylation.
This altered metabolism boosts the adoption of a compensatory and alternative pathway to generate energy in cancer cells.
The Warbur effect seems to help tumor cells counteract high levels of ROS, as a result of high glucose concentrations in tumor microenvironment increased production of lactate and glutathione, promoting alternative strategies to generate energy and leading to accumulation of reactive oxygen species.

Cancer cells are characterized by mutations in oncogenes, such as IGF-1 receptor (IGF-1R), the GTP proteins RAS/RAF, mitogen-activated protein kinase (MAPK), phosphatidylinositol 3-kinase (PI3K), the transcription factor c-Myc, which play the roles of coordinators in progression and proliferation independently or partially independently of external growth factors (Buono et al., 2018). In addition, cancer cells show insensibility to inhibitory signal due to loss of function mutations in tumor suppressor genes (*e.g.* p53, p21, PTEN) (Bianchi et al., 2015).

The loss of function of p53 or mutation in genes involved in DNA repair could be associated to a difference in radiation sensitivity. Dysregulation in cell cycle arrest is a relevant event in the response to radiation, because the G1/S and G2/M checkpoints are activated to provide time for DNA repair. Dysregulation in this mechanism causes an inefficiency or an incomplete DNA repair. The difference in cell cycle kinetics induced by diets or food intake in normal and in cancer cells could show a divergent DNA repair and response to IR, resulting from cancer gene instability (Shi et al., 2012).

Furthermore, hypoxic conditions could increase the cancer cell dependence to glycolysis. The expression of hypoxia-inducible transcription factor 1a (HIF-1α) and HIF-2α, induce the upregulations of glucose transporter, glycolytic enzyme, and expression of stem cell genes. As described by Béclèr in 1901, hypoxia influences radiosensitivity of tumors.

The understanding of molecular pathways and metabolism deregulation in tumors and its intervention changing may provide an improvement of radiotherapy.

For this reason, we hypothesize that short-term starvation can increase the efficacy of radiotherapy on cancer cells.

1.6. Combining short-term starvation to enhance the anti-tumor effects

The standard cancer treatment, chemotherapy and radiotherapy, even though their efficacy, are characterized by several side effects. Recent studies have elucidated as nutrient modulation through diet or geroprotective dietary regimens, may sensitize cancer cells to treatment and protect normal cells (Di Biase et al., 2017; Klement et al., 2018).

Several studies demonstrated that fasting or short-term starvation (STS) can selectively protect normal cells, mice and potentially patients from chemo-toxicity without reducing the therapeutic effect on cancer cells (Brandhorst et al., 2017). This phenomenon was termed by Sadfie *et al.* as Differential Stress Resistance (DSR) and is based on the hypothesis that normal cells will enter an alternative metabolism state, during STS, characterized by the redistribution of cellular energy from reproduction/growth to protection/maintenance program. Instead cancer cells, characterized by constitutive activation of proliferative pathways causing by mutations in oncogenes and tumor suppressor genes, are unresponsive to DSR (Lee et al., 2011).

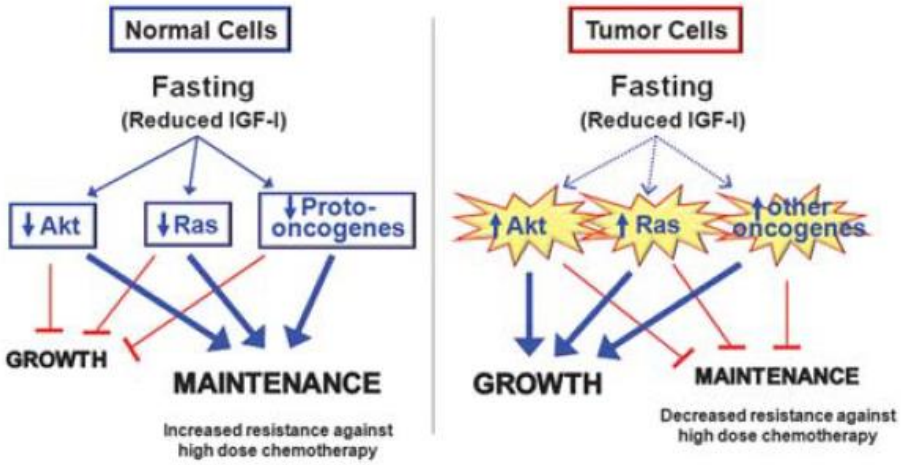

Figure 4: Mechanism of Differential Stress Resistence in normal and tumor cells (Lee et al., 2011).

Evidences from preclinical studies demonstrate that fasting reduces plasma levels of growth factors, insulin-like growth factor-I (IGF-I) and modulate intracellular metabolism signal rendering cancer cells more vulnerable to chemotherapeutics (Lettieri Barbato et al., 2018).

In the last years, several randomized trials based on preclinical results were designed to test the efficacy and the effect of chemotherapy on both normal and cancer cells after a fasting cycles (Longo et al., 2014).

A summary of clinical trials in which short-term starvation, intermittent fasting, or fasting-mimicking diets, in combination with anticancer therapies are listed in **Table 1**.

Dietary Intervention	Clinical trials	Status	Disease	Enrollment (participants)	Study (first author)
Short-term fasting	NCT01175837	Active, not recruiting	Malignant Neoplasm	12	No results posted
Short-term fasting	NCT01304251	Completed	Breast Cancer	13	De Groot *et al*., 2015 Safdie *et al*., 2009
Short-term fasting	NCT00936364	Recruiting	Solid Tumors	70	Dorff *et al*., 2016
Fasting mimicking diet	NCT02126449	Recruiting	Breast Cancer	250	No results posted
Low calorie diet	NCT01802346	Recruiting	Breast Cancer, Hormone-resistant Prostate Cancer, Recurrent Prostate Cancer	120	No results posted
Fasting	NCT01954836	Completed	Cancer	50	Bauersfeld *et al.*, 2018
Fasting	NCT02710721	Recruiting	Prostate Cancer	60	No results posted
Starvation	NCT02607826	Not yet recruiting	Cholangiocarcinoma Pancreatic Ductal Adenocarcinoma Colorectal Cancer Gastric Cancer Adenocarcinoma of the Esophagogastreal Junction Esophagus Cancer	298	No results posted

Table 1: List of ongoing or completed clinical trial with diet intervention.

The first preliminary clinical data were collected as a part of different pilot studies to assess the safety and feasibility of short-term fasting prior to administration of chemotherapy (NCT01175837). One of the first randomized pilot study (NCT01304251), was planned to establish the safety and tolerance of short-term fasting with chemotherapy in early breast cancer patients. Due to limitations of this studies, such as small sample size and lack of stability in statistical analysis, larger randomized trials such as the DIRECT study (NCT02126449), will provide new data on possible benefits of short-term fasting in cancer patients.
Other randomized clinical trials are been conducted to demonstrate the reduction of side effects in patients receiving gemcitabine hydrochloride and cisplatin for advanced solid tumors (NCT00936364), gynecological cancer disease, ovarian, breast and prostate cancer (NCT01802346, NCT01954836).

In particular, the NCT02710721 study had the scope to evaluate if in CRPC castration-resistant prostate cancer or hormone-sensitive prostate cancer patients with metastatic disease, an intermittent fasting could improve quality of life, limit side effect and reduce tumor progression. Other randomized clinical trials are needed to support the efficacy of short-term starvation in cancer.

This study could suggest if simultaneous STS or fasting during radiotherapy could be a novel approach to improve the therapy's efficacy, limit side effect and preserve healthy tissue.

1.7. Cancer and Radiotherapy

In the recent years, the use of high-dose single fraction therapy in control of local tumor and metastases has achieved a growing number of impressive results. Several studies using a single dose or up to 3 large fractions radiotherapy have been published for lung cancer, liver metastases, brain metastases, spine metastases, kidney and pancreatic tumors, demonstrating an improvement in control diseases (Brown et al., 2008; Kennedy et al.,2017).

In the field of preclinical oncology, research groups have recently displayed as the combination of intermittent fasting, a form of caloric restriction, and chemotherapy could improve therapy beneficial effects and prevent side-effects.

At present, a small number of data are available on the effect of short-term starvation and radiotherapy. This lack, probably, is due to the complication to combine patients diets and radiotherapy treatment, furthermore plan a rigorous clinical trial. On the basis of previous consideration, we decided to focus on high-dose single-fraction radiotherapy and to the use of cell lines derived from spinal lesions, from pancreatic tumor's liver metastases and lung cancer. According to this set of single dose session, a fasting period of 24 hours before radiotherapy is feasibility.

Below a listed of cancer disease in which high dose single radiotherapy illustrate a powerful clinical approach compared to multiple-dose low fractions.

1.7.1. Lung cancer

Lung cancer is the leading cause of cancer death in the United States. Non–small cell lung cancer (NSCLC) accounts for 85% of all lung cancer cases and the most common type of NSCLC is adenocarcinoma (40%). The standard treatment for patients with advanced NSCLC has been chemotherapy, but more recent progress in molecular biology allowed the identification of several numbers of mutations, opening a scenario for personalized therapy.

In the last years, the accelerated hypofractionated radiotherapy and SBRT in case of advance cancer, inoperable lung cancer (McCloskey et al, 2013; Slotman et al., 2014) or elderly patients that cannot receive the standard of care, are considered as an alternative option to conventional regimen (Chua et al., 2017; Tekatli et al., 2016). Despite rapid advancements in molecular biology research, the prediction of treatment response in lung cancer still remain a great challenge.

Approximately 50% of lung adenocarcinomas harbor TP53 tumor suppressor gene mutation. Several retrospective and meta-analysis studies demonstrate that the p53 mutations status is a significant predictor of poor outcome in patients with lung cancer (Ahrendt et al., 2003). P53 is implicated in several signal pathways, such as the induction of genes associated with DNA repair, cell cycle regulation, oxidative stress response and apoptosis regulation. Currently, no adjuvant therapy or biological approaches could produce a survival benefit, therefore new approaches are desirable. Apontes *et al.* demonstrated that the induction of p53 with anti-diabetic drug determined a cell cycle G1/G2 arrest in normal cells and not in mutant p53 cancer cells, protecting them from microtubule active inhibitors and cell cycle-specific chemotherapeutic agents. We supposed that short-term starvation characterized by low blood levels of nutrients (*e.g.* glucose, amino acids, insulin) protect normal tissue from side effect of radiotherapy and define an effective improve combination in adenocarcinoma with mutant p53.

In perspective to precision medicine, we hypotized that tumor-related mutation, such as p53, in association with short-term starvation could influence the response to radiotherapy.

1.7.2. Metastatic prostate cancer

Prostate cancer is the fifth leading cause of death and the most common cancer among men. Prostate cancer often develops in a not responsive androgen deprivation therapy called Castration-Resistant Prostate Cancer (CRPC). CRCP is associated with 80% bone metastasis, with the spine the most common metastatic site. The pain and neurologic complications of vertebral metastasis alter the quality of life in CRCP patients. Treatment approaches for prostate spinal metastasis include a multidisciplinary approach as surgery, chemotherapy, hormone treatment, radioisotopes and radiotherapy. Radiotherapy is recommended to constant pain, spinal cord compression and inoperable pathological fractures. One of the emerging therapy for treatment of spinal mCRPC is stereotactic radiosurgery (SRS) (Scott et al., 2004). The stereotactic body ration therapy (SBRT) is characterized by high dose of radiation delivered in a few fractions in a total period of 5-10 days. The assessment and management of patients with spinal metastasis are complex due to the presence of adjacent critical organs (*e.g.* spinal cord, esophagus, bowel) and required a multidisciplinary team, involving radiation oncology, spine surgery, medical oncology and radiology. Anyway spine SBRT is a highly effective treatment due to improvement in patient immobilization, target visualization, and image guidance that had permitted the delivery of ablative doses to the target avoiding critical organs (Tseng et al., 2017). Currently, the spine SBRT is becoming an efficient option for the treatment of spinal oncological lesions, anyway the setting of ideal dose fractions and

an appropriate guidelines practice is at present uncertain (Gonzales Ruiz de Léon et al., 2017; Rao et al., 2017).

1.7.3. Metastasis of pancreatic cancer

Pancreatic cancer is still one of the oncological diseases with the worth prognosis. The early diagnosis is still difficult due to the lack of clear or peculiar symptoms in patients, to the absence of specific and sensitive markers for detection and to complexity of image instrumental detection (Neoptolemos et al., 2018).

When pancreatic cancer is diagnosed, many patients are already in advanced stage of metastases with dissemination in retroperitoneum, vascular system and nerves. The most frequent type of metastases are in liver and peritoneum. The overall survival (OS) of patients with metastatic disease remains less than 11 months. The therapeutic regimes consisted, only for a subset of patients, in a resection of both tumor (primary and metastasis), and for all other in a palliative chemotherapy (Yamada et al., 2006). Pancreatic liver metastases are not resectable in most case. Clinical trials studying SBRT and chemoradiation approach are limited, and the lack of solid data, due to biased published patient cohorts data, invalidate an established guideline (Crane, 2016; Ouyang et al., 2011).

The positive results of these studies indicate that a subgroup of patients with pancreatic metastatic disease may prolong survival when treated with a multimodal treatment consist of surgical resection and chemo-radiation (De Bari et al., 2016; Ikeda et al., 2001; Scorsetti et al., 2011).

New future directions to improve the efficacy of neo-adjiuvant treatment, to overcome the issue of toxicity risk and subsequent damage to critical organs and to deliver ablative doses safely for pancreatic cancer are need.

Here we investigate if a multimodal approach including diet, could be useful to enhance the effect of radiotherapy.

Material and Methods:

Cell lines

A549 (adenocarcinoma cell derived from primary lung cancer), MRC-5 (normal fibroblast lung cell lines), VCaP (prostate cancer cell derived from vertebral metastatic site) and CFPAC1 (pancreatic cancer cell derived from liver metastatic site) were obtained from the American Type Culture Collection (ATCC, Rockville, MD). A549sip53 (silenced for p53) were kindly donate and silenced by Dott. Bossi.

Cell lines were maintained in DMEM supplemented with 10% FBS and 1% L-glutamine (Euroclone, Milan, Italy) at 37°C.

The oxygen partial pressure (pO_2) plays a fundamental role in the molecular and metabolic features of cells, and in the response to ionizing radiation. For this reason the cells were maintained in hypoxic conditions, in order to get as close as possible to the physiological microenvironment.

In vitro radiation system

The flasks, 96-multiwell plates containing monolayers cells or 3D-spheroids were inserted into a custom built plexiglass phantom (40 × 40 × 8 cm). The phantom was irradiated using a 6-MV photon beam delivered by an Elekta Synergy linear accelerator (Elekta Oncology Systems, Stockholm, Sweden). The delivered dose was calculated using the Philips Pinnacle 3 radiation therapy planning system (Philips Healthcare, DA Best, The Netherlands) customized with the geometric and dosimetric characteristics of an Elekta Synergy linear accelerator, as previously described (Tesei et al., 2013).

Treatments

STS Treatments. Glucose restriction was done by maintaining cells in glucose-free DMEM (Invitrogen) supplemented with either low glucose (0.5 gr/liter) and 1% FBS for 24 hours (Raffaghello et al., 2008).

Radiation. Cells were irradiated in 25-cm^2 flasks or 96-multiwell plates using the linear acceleration Elekta Synergy Platform system. Cell lines were treated with a combination of STS followed by radiation treatments. The delivery dose used was 5 Gy for lung cell lines, 8 Gy and 10 Gy for metastatic cell lines (VCAP and CFPAC-1, respectively).

In vitro Cytotoxicity assay

Cell viability assay was performed with CellTiterGlo (Promega, Milan, Italy) according to manufacturer's protocols. Briefly, 5000 cells were cultured in a 96-well plate. CellTiter-Glo reagent was added in each well, and mixed for 2 minutes to induce cell lysis. After 10 minutes incubation at room temperature, the luminescent signal was recorded using Glomax (Promega, Milan, Italy).

3D cell viability was measured using CellTiter-Glo® 3D Cell Viability Assay (Promega, Milan, Italy). Spheroids were removed from the 96-well low-attachment culture plate and placed separately in single wells of a 96-well opaque culture plate (BD Falcon). CellTiter-Glo® 3D reagent was added to each well and the luminescence signal was read after 30 minutes with the GloMax® bioluminescent reader (Promega, Milan, Italy).

Clonogenic assay

Following treatment, 500 cells were seeded in 10 cm^2 dishes in 500 ml of medium. After 14 days, the resulting colonies were fixed and stained using 0.5% crystal violet in 25% methanol; colonies with more than 50 cells were quantified under inverted microscope (I500X, Olympus) by two independent observers. Five series of samples were prepared for each treatment dose.

Flow cytometry

Flow cytometric acquisitions were performed using a FACS Canto flow cytometer (Becton Dickinson, San Diego, CA). Data were analyzed by FACSDiva software (Becton Dickinson, San Diego, CA) and ModFit 2.0 (DNA Modelling System, Verity Software House, Inc., Topsham, ME). Samples were run in triplicate and 10,000 events were collected for each replica. Data were the average of three experiments, with errors under 5%.

Cell cycle distribution. After each treatments, cells were fixed in 70% ethanol, stained with propidium iodide (10 mg/ml, MP Biomedicals, Verona, Italy), RNAse (10 kunits/ml, Sigma Aldrich) and NP40 (0.01%, Sigma Aldrich) overnight at 37 °C in the dark and analyzed by flow cytometry. Data were expressed as fractions of cells in the different cycle phases.

Tunel. TUNEL assay was performed using In situ Cell Death Detection Kit, Fluorescein (Roche Applied Science, Indianapolis, IN).Cells were fixed in 4% paraformaldehyde and resuspended in permeabilization solution (0.1% Triton-X100, 0.1% sodium citrato in PBS) for 10 minutes on ice. The cells were labeled with reaction solution composed by Tdt enzyme and FITC-labelled nucleotides. A negative control without addition of Tdt enzyme and positive control treated with DNase I were included. After incubation for 60 minutes at 37°C, the samples were analyzed by flow cytometry.

Immunofluorescence staining

Cells were harvested by trypsinization, washed with serum and PBS1X and plated onto glass coverslips. The cells were fixed with paraformaldehyde for 15 minutes on ice.

The coverslips were incubated overnight at 4°C in primary antibody (anti Rad51 diluted 1:100, Cell Signaling, Danvers, MA; anti-γH2AX), diluted in blocking buffer, and then washed again with PBS1X and incubated with fluorochrome-conjugated secondary antibodies (FITC green, Alexafluor 488 goat, Life Technologies) for 2 h at room temperature. Cells were analyzed with Zeiss Imager M1 microscope (Zeiss, Milan, Italy) and the images were recorded with Zeiss AxioVision camera. A minimum of 100 cells were analyzed for each experiment and the cells containing a minimum of five RAD51 and γH2AX foci per nucleos were scored as positive. An automatic focus scoring were performed using the cell image analysis software, Fuji ImageJ. All image analysis parameters were kept constant throughout the duration of experiments.

Comet assay

The alkaline comet assay was performed according to the manufacturer's protocol (Comet assay, Trevigen, Gaithersburg, MD). Briefly, at the end of the treatments, 5000 cells were suspended in LMAgarose (at 37 °C) and were immediately transferred onto the comet slide. The slides were immerged for 1 h at 4 °C in a lysis solution, washed in the dark for 1 h at room temperature in an alkaline solution, and electrophoresed for 30 min at 21 Volt. Slides were then dipped in 70% ethanol and stained with the Syber green (Bio-Rad Laboratories, Hercules, CA, USA).

One hundred of comets from category 0 to category 4 were selected and the image were capture using EVOS microscope at 10x magnification.

The DNA damage is quantified by computing, in single cells, the displacement between the genetic material contained in the nucleus, typically called "comet head", and the genetic material in the surrounding part, considered as the "comet tail". To obtain reproducible and reliable quantitative data, we developed an easy-to-use tool named *CometAnalyser*.

Today, a few freely available tools exist to analyse microscopic images acquired with a comet assay. The two most known are *OpenComet* and *CometScore*. Gyori *et al.* developed *OpenComet* as a plug-in for *ImageJ*. The tool can be used for the analysis of both fluorescent and silver stained images. The segmentation of the comet's border is based on geometric shape attributes, whilst the segmentation of the comet head is obtained through an image intensity profile analysis. *CometScore* is an open-source tool freely available at: http://rexhoover.com/ (freeware v1.5). Using *CometScore*,

the expert selected the comet boundary and indicated its head centre manually. The parameters are then automatically calculated by the software. These tools typically work well in case of fluorescent images and, in general, ideal images. However, segmentation errors increase in case of noisy images like the silver staining ones (Ganapathy et al., 2016), usually presenting debris and vignetting effect (Piccinini et al., 2012), or in case of images with cells characterized by different morphologies. Several commercial tools are also available (for a list of commercial comet assay analysis tools see: www.cometassay.com), but they are costly and do not provide possibilities for examining the code and modifying the processing algorithm.

CometAnalyser is a semi-automatic tool developed with the goal to be extremely user friendly. It has been developed in *MatLab* (The MathWorks, Inc., Natick, MA, USA) and the current version (*CometAnalyser* v0.9) requires *MatLab R2017b* and the *MatLab Image Processing Toolbox 10.1*, or a later version. *CometAnalyser* works with silver staining and fluorescent images. The working procedure can be briefly summarized in three main steps. (*a*) First of all, the user has to draw with the mouse a region surrounding the cells of interest. The tool then automatically segments comet heads and nuclei. By default, the Otsu thresholding segmentation method is used (Otsu, 1979), but other algorithms are available and several parameters can be then modified to adjust the segmentation. (*b*) Once the comets have been segmented, Tail Moment and all the other features listed by Gyori *et al*. are automatically computed and saved as *Excel* file. (*c*) Snapshots of all the segmented comets are stored in different folders according to a classification currently manually performed by the user. Finally, the project with all the labels can be saved and loaded back for future modifications.

Three-Dimensional Cell Culture

A rotatory cell culture system (RCCS) (Synthecon Inc., Houston, TX, USA) was used as previously described (Tesei et al., 2013). The rotator bases were placed inside a humidified 37 °C incubator and connected to power supplies set up externally. Single cell suspensions of about 1×10^6 cells/ml of lung cell line were placed in the 10-ml rotating chamber at an initial speed of 12 rpm. The culture medium was changed every 4 days and tumor spheroids with an equivalent diameter ranging from about 500–700 μm (depending on the cell line used) were obtained in around 15 days. The spheroids were transferred into 96-well low-attachment culture plates (Corning Inc., Corning, NY, USA).

Morphological analysis of 3D tumor cultures

Growth and morphology of the 3D tumor colonies were monitored for several days as regards changes in area, volume and shape. Phase-contrast imaging and morphological analyses of spheroids were carried out with an inverted Olympus IX51 microscope (Olympus Corporation, Tokyo, Japan), equipped with a Nikon Digital Sight DS-Vi1 camera (CCD vision sensor, square pixels of 4.4 μM side length, 1600 × 1200 pixel resolution, 8-bit grey level) (Nikon Instruments, Spa. Florence, Italy). The open-source AnaSP29 and ReViSP30 software tools (Piccinini et al., 2015) were used to achieve morphological 2D (*e.g.* diameter, perimeter, area) and 3D (*e.g.* volume, sphericity) parameters, and to select morphologically homogeneous spheroids as previous described (Zanoni et al., 2016).

Real-time Quantitative Polymerase Chain Reaction (RT-qPCR)

Total RNA was extracted from cell lines using TRIzol® reagent following the manufacturer's instructions (Invitrogen). Reverse transcription (RT) reactions were performed in 20-ul volume containing 400 ng of total RNA using an iScript TM cDNA Synthesis kit (Bio-Rad Laboratories, Hercules, CA, USA). The mRNA levels of the selected genes were assessed by real-time quantitative PCR (RT-qPCR) using costum TaqMan probes (Applied Biosystems, Carlsbad, CA) and an ABI7500 system. Probes were selected from inventoried gene expression assays (Invitrogen, Thermo Scientific).

The comparative threshold cycle (Ct) method was used to calculate the relative gene expression. The gene target expression was normalized to an endogenous reference Beta-actin. Reference genes were chosen using the geNorm VBA applet for Microsoft Excel to determine the most stable reference genes. Relative quantification of target gene expression was calculated using the comparative Ct method. All experiments were conducted in triplicate.

Western blot analysis

Cells were treated according to the previously described Western blot procedure (Pignatta et al., 2014). The following antibodies were used: goat anti-rabbit IgG-HRP: sc-2004 1:5000 (Santa Cruz Biotechnology, Santa Cruz, CA, USA), anti-vinculin 1:1000 (Invitrogen, Thermo Scientific), Precision Protein™ StrepTactin-HRP Conjugate 1:10,000 (Bio-Rad Laboratories, Hercules, CA, USA), anti-p53 1:1000 (Cell Signaling Technology, Inc., Beverly, MA, USA). Densitometric analysis was performed using Quantity One Software Version 4.6.7. (Bio- Rad Laboratories).

3. Results

3.1. Silencing p53 in adenocarcinoma cell lines reduces sensitivity to radiation

Two adenocarcinoma lung cancer cell lines were used in this study. One, A549, that expresses functional wild-type p53, and the other one, A549sip53, p53 silenced. First we checked the silencing of p53, evaluating the mRNA and protein expression. We observed, compared to A549, a substantial downregulation of p53 transcript and protein **(Fig1, A-B)**.

The proliferation potential and radiosensitivity of A549 and A549sip53 were measured using clonogenic assay, after cells exposure to conventional IR treatment. The conventional treatment consists of 2Gy dose per fraction delivered daily over 24 days to a cumulative dose of 48 Gy. The cells were irradiated using a 6-MV photon beam delivered by an Elekta Synergy linear accelerator (Elekta Oncology Systems), the same machine used on a daily basis to deliver radiotherapy to patients.

We found that the expression of p53 affects the response to radiation, resulting as shown in **Figure 1C**, in a considerable reduction in colony formation respect to p53 silenced cell line.

A rotary cell culture system (RCCS) was used to produce 3D-spheroids culture. Spheroids were exposed to hypofractionate IR (5Gy dose per 5 fraction) to evaluate the proliferation potential and radiosensitivity in 3D structure. As shown in **Figure 1D**, the IR resistance of A549sip53 is maintained also in 3D-spheroids.

3.2. Effect of short-term starvation on cell cycle

A549 (wt p53), A549sip53 (silencing for p53), MRC-5 normal fibroblast lung cell lines and CFPAC1- VCaP (metastatic cell lines) were tested for short-term starvation. Cells were incubated in low glucose STS - short term starvation medium (0.5gr/l glucose + 1% FBS) or in control standard DMEM medium (1gr/l glucose + 10 % FBS) for 24h and cell cycle distribution were analyzed by flow cytometry.

STS resulted in a higher disturbance of cell cycle distribution in MRC-5 fibroblast cell lines compared to cancer cell lines. As shown in **(Fig. 2A)**, an increase of 20% of cells in the G0/G1 phase was observed in STS MRC5 with a concomitant reduction of cell percentages in S-phase and G2/M phases (73% and 29%, respectively), compared to MRC5 cultured in control medium.

Regarding tumor cell lines, the depletion of nutrients determined a moderate increase in the percentage of cells in G0/G1 phase, rising of 10% in all cell lines. The diminution of S-phase fraction in cancer cells ranged from 10% to 43% **(Fig. 2B-E)**. A549 was the only cancer cell line characterized by a drop of G2/M phase after STS **(Fig.2B)**.

Instead, in metastatic pancreatic cancer cell line CFPAC1, the starvation condition did not drastically affect cell cycle distribution, with a change in all phases distribution of about 10% **(Fig.2D)**.

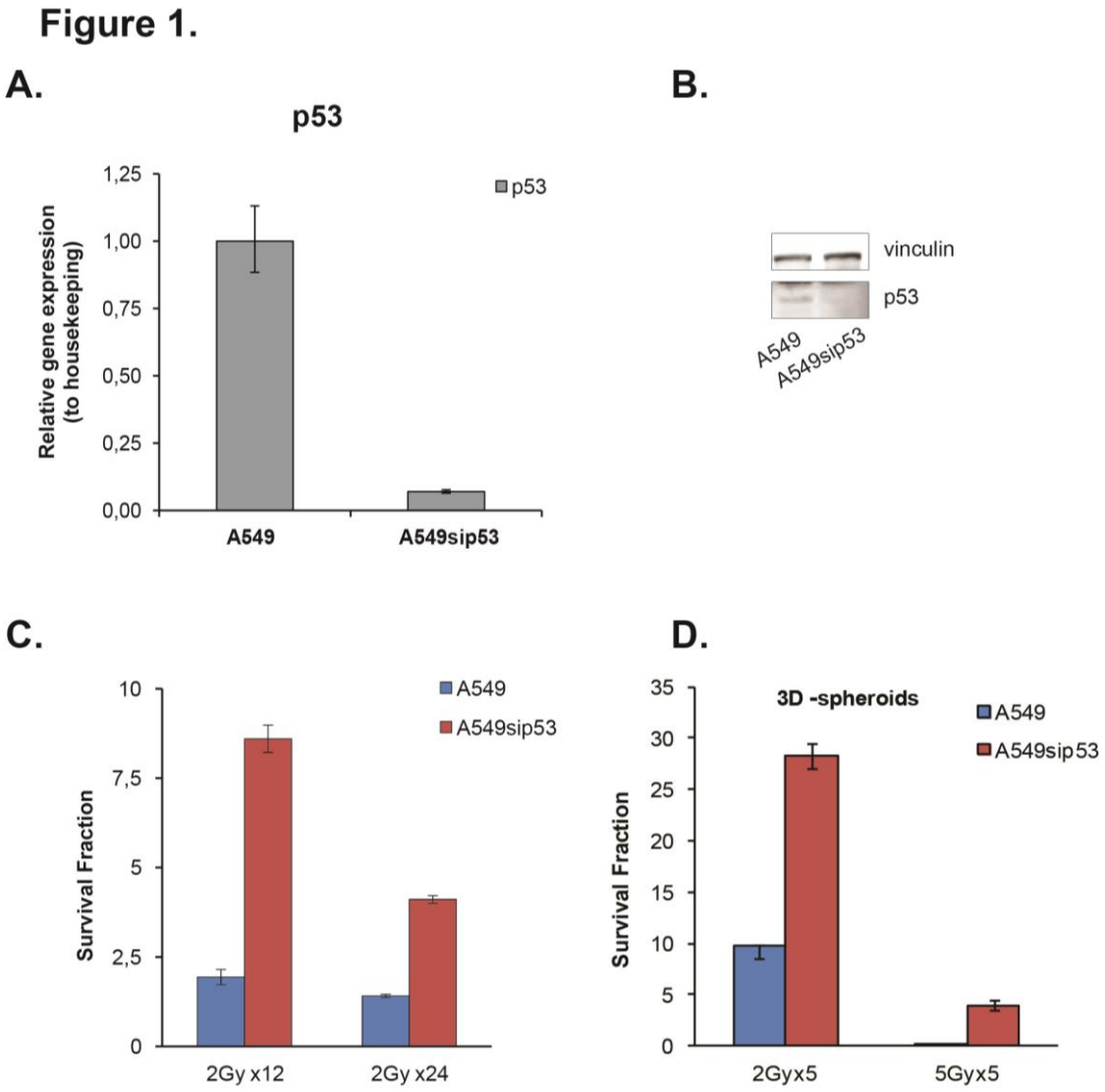

Figure 1: Effect of p53 silencing on radiation response cells. (A) p53 mRNA expression in lung adenocarcinoma cell lines were assessed by real-time quantitative PCR. The results were normalized to housekeeping and are presented as the mean ± SD of three independent experiments. (B) The p53 protein levels were measured by western blotting analysis. Vinculin was used as a loading control. (C) The radiation response was determined by colony formation assay. Data point are represented as mean ± SD.

Figure 2.

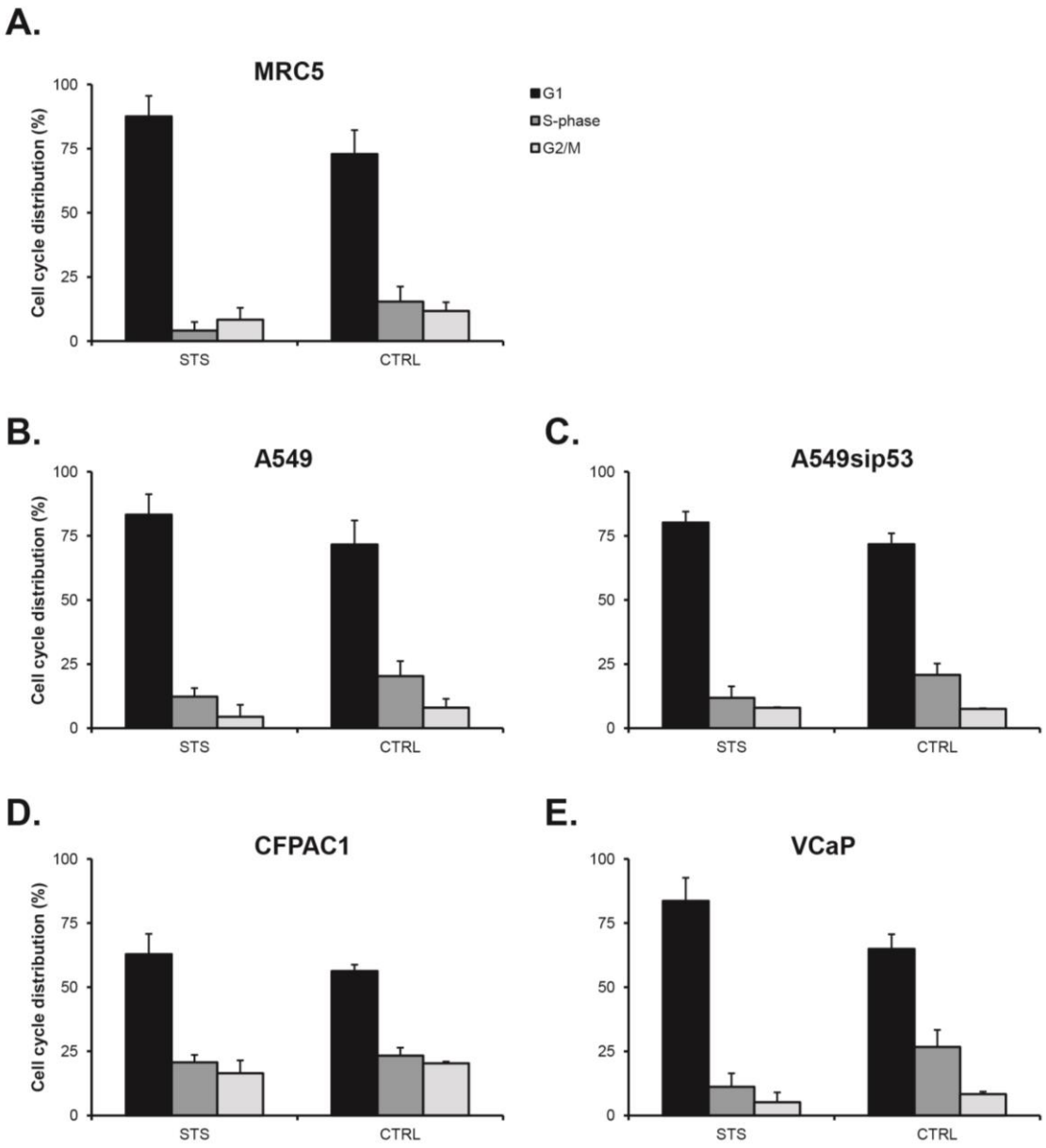

Figure 2: Cell cycle distribution after 24h of short-term starvation. (A-E) Histograms G0/G1, S-phase and G2/M indicate the distribution of cell populations in each phase of the cell cycle. Data are reported as mean ± SD, for three experiments.

3.3. Cell viability assay in starved and non-starved cancer cell lines

As a first step we performed a dose response curve to establish the effect of radiation on cells in short-term starvation (STS) or in control standard medium (CM). Cell viability rate is measured at 72 hours. We observed that radiation caused 50% of cell death in MRC5, A549 and VCaP cell lines (**Fig.3, A, B, E)**. Moreover, the differences between the radiation alone and combined with STS were not statistically significant ($P \geq 0.05$), denoting that STS had no effect on cell death rate after 72h in these cell lines.

The radiation treatment in A549sip53 caused only 20% of cell death at 72h **(Fig. 3C**), indicating that the A549 cell lines p53 silenced are more radio-resistant than A549 wild type.

Only the metastatic pancreatic cancer -cells (CFPAC1) displayed a cell death rate of 90% with radiation treatment **(Fig. 3D)**. Furthermore, combining IR with STS, the induced inhibition of cell viability was statistically significant ($P \leq 0.05$) compared to IR alone.

3.4. Cell cycle arrest under the influence of RT

Since RT prevent cell growth, proliferation and DNA synthesis, we then performed a cell cycle analysis to test whether RT influence cell cycle arrest. Moreover, we compared the cell cycle distribution of cells cultured in CM or STS. RT combined with STS treatment induce in MRC5 cell lines **(Fig. 4A)** an increase in the percentage of cells in G0/G1 phase with a parallel decrease of S-phase population. In particular, when we treated MRC5 cell lines with RT and STS, we observed a missing of S-phase and a reduction of G2/M phase compared to RT alone.

Figure 4B-C shows how STS determined in both A549 and A549sip53 cell lines, a slight increment of G0/G1 phase and a reduction of S-phase. Anyway, we observed unsubstantial variations of cell cycle phases after IR exposure in combination or not with STS. The percentage of cells in cell cycle phases after IR remain unvaried.

Instead, as shown in **Fig. 4D-E**, we observed a dramatic perturbation of cell cycle in metastatic cell lines (CFPAC1 and VCaP) after RT treatment, characterized by a drop-off in G0/G1 population associated with an increase of G2/M phase. These cell cycle perturbations are related to the mechanism of action of irradiation and hide the effect of STS alone. This suggests that the majority of the effects observed in these experiments is due to irradiation treatment.

Figure 3.

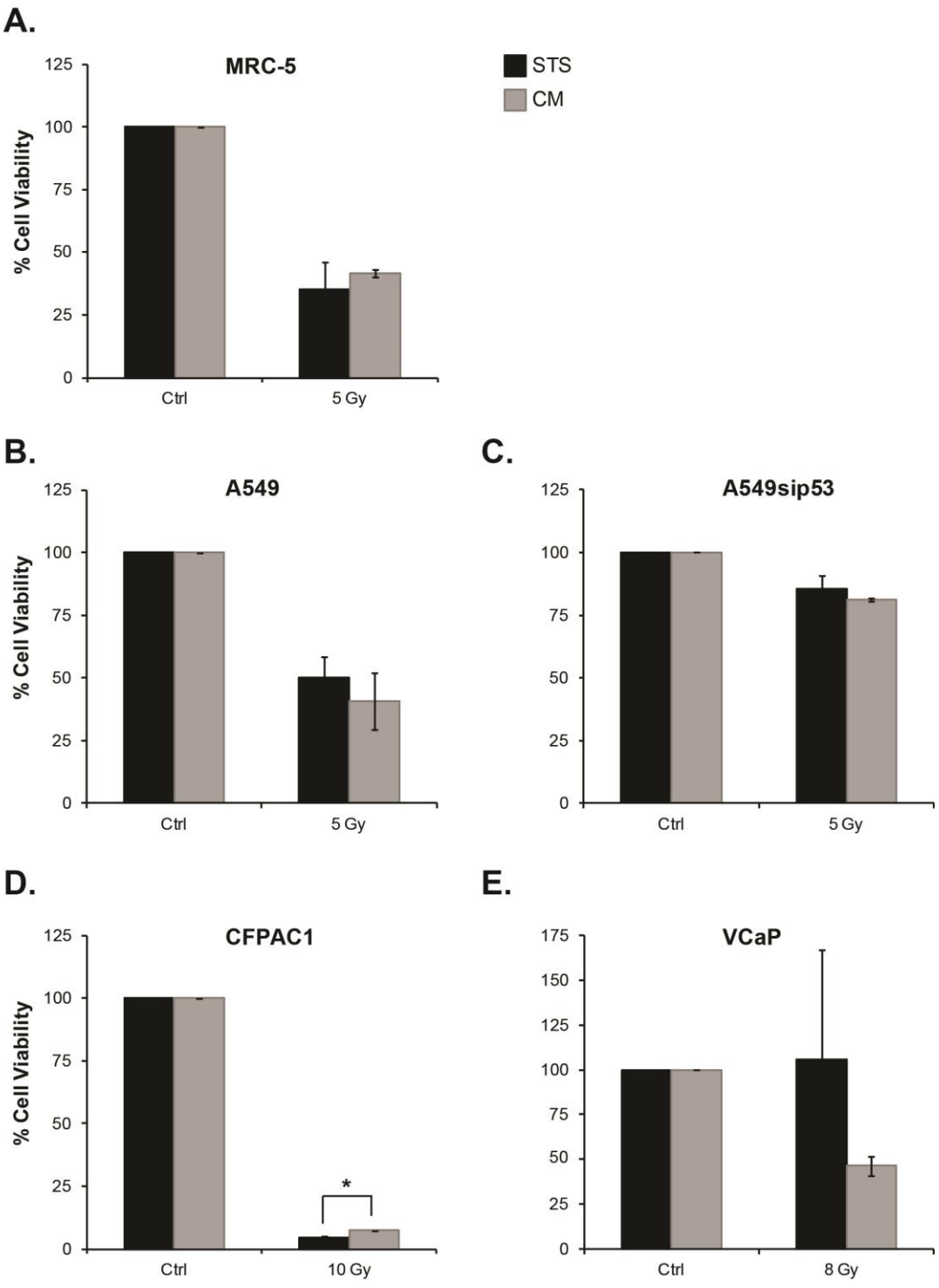

Figure 3: Effect of IR on cell viability. Cells (MRC-5, A549, A549sip53, CFPAC1 and VCaP) were exposed to ionization radiation in normal medium (CM) or in short-term starvation medium (STS). The cell viability was evaluated using CellTiter Glo after 72h from the end of IR. Data are reported as the mean ± SD for three separate experiments performed in octuplicate. (*$P < 0.05$)

Figure 4.

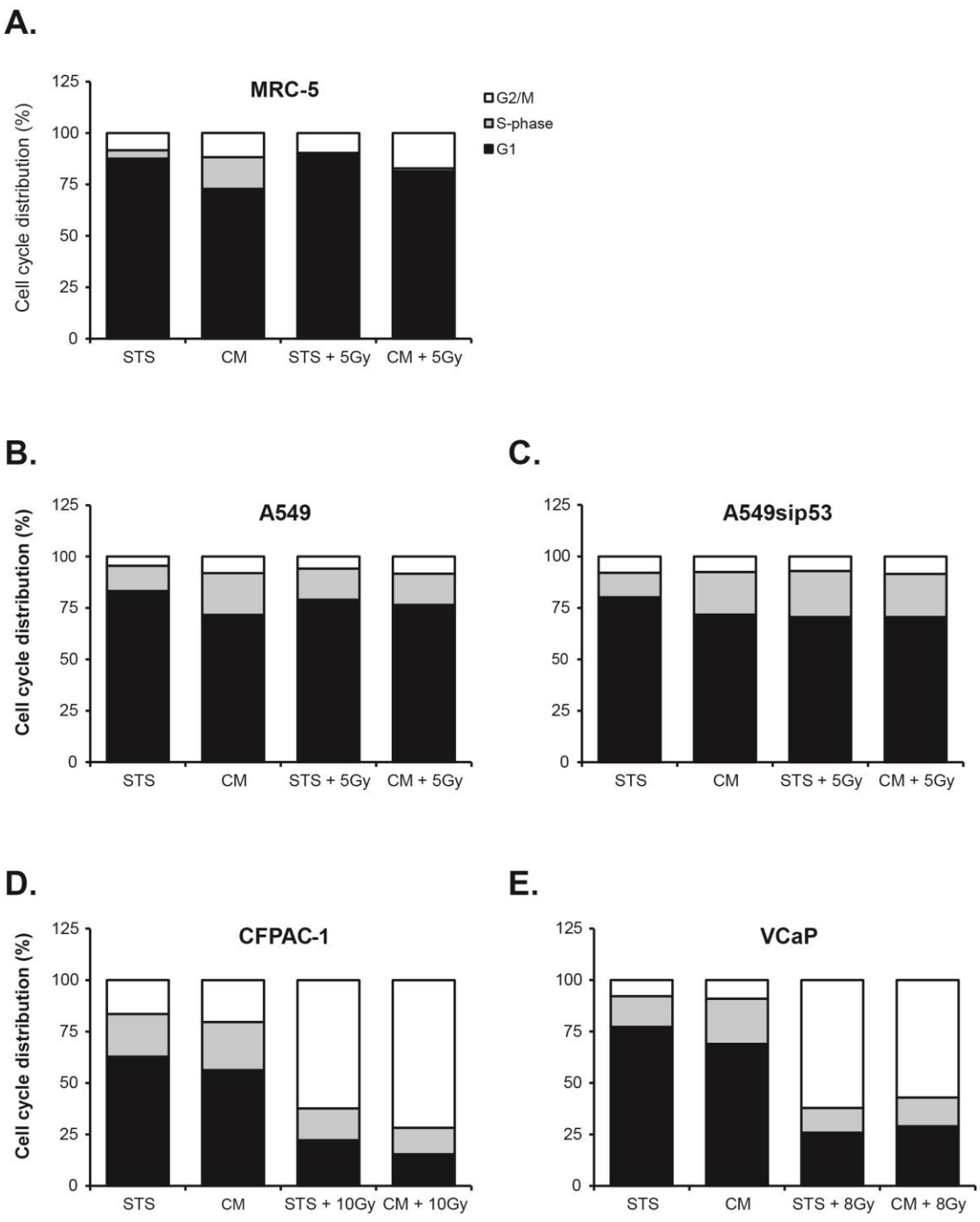

Figure 4: Impact of RT and STS on cell cycle distribution. Cells were exposed for 24h to STS or CM medium and then treated with RT. Cell cycle was analyzed after 72h by flow cytometry. Histograms G0/G1, S-phase and G2/M indicate the distribution of cell populations in each phase of the cell cycle.

3.5. Clonogenic assay

After an initial curative treatment, in cancer patients often occurs the re-growth of tumor due to a small number of cells that retain colony-forming ability. This phenomenon is associated with a poor clinical outcome. We performed colony formation assays to evaluate the long term response and the colony forming ability of the different cell lines exposed to RT and STS.

Cells were incubated in STS or CM for 24h and treated with a single dose of 5Gyx1 (lung cancer cell line), 10Gyx1 (metastatic prostate cancer cell line) and 8Gyx1 (metastatic pancreatic cancer cell line) on the basis of clinical data **(Fig.5)**. The clonogenic assay was fixed after 15 days.

The surviving fraction of A549 (wt p53), A549sip53 (p53 silenced), MRC-5 normal fibroblast lung cell lines, VCaP (prostate cancer cell derived from vertebral metastatic site) and CFPAC1 (pancreatic cancer cell derived from liver metastatic site) was evaluated.

STS for 24h before RT caused a significant radiation sensitizing effect in metastatic cell lines CFPAC1 and VCaP **(Fig.5D-E)**, with a complete inhibition of proliferation potential in VCaP. We also found that radiation effect was significantly not enhanced by STS in normal cell lines MRC5, denoting that STS could protect normal tissue by IR damage. **(Fig.5A)**

Furthermore, a significant difference in surviving fraction was observed also in A549 where RT was combined with STS **(Fig. 5B).** Counterwise, due to their basal radioresistance, in A549sip53 cells the radiation effect was not as profound as seen in A549 and no significant change in surviving fraction between the different culture nutrient conditions was observed **(Fig. 5C).** All together these data show that p53 mutation status do not influence the effect of short-term starvation on radiosensitivity in tested adenocarcinoma cell lines.

Figure 5.

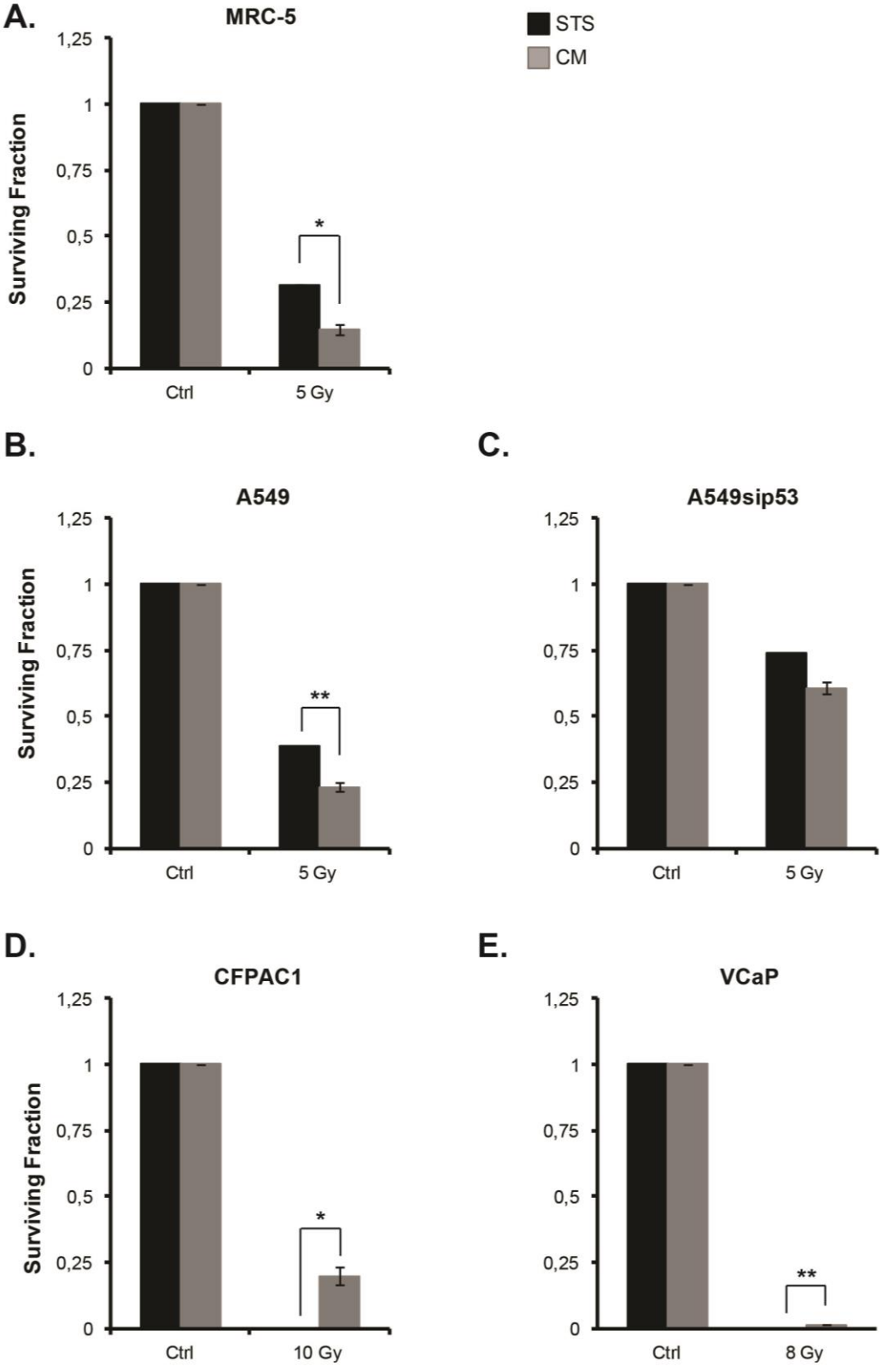

Figure 5: Clonogenic assay (n=12) were analyzed for cell lines treated with RT in CM or STS. The data shown are the mean values (±SD) from independent experiments. Statistical significance *p < 0.05, **p<0.01.

Figure 6.

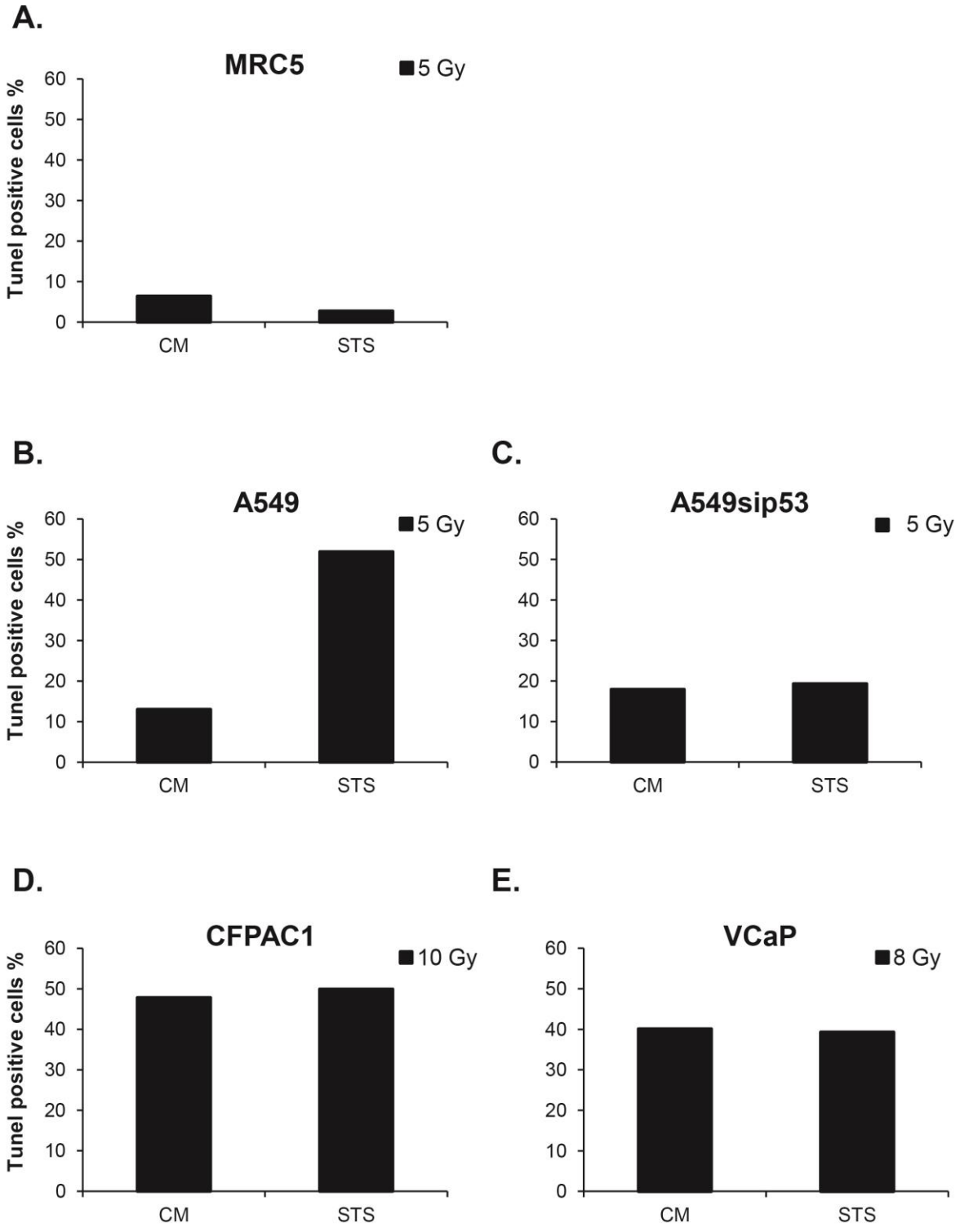

Figure 6: Apoptosis was assessed by TUNEL. Quantification of TUNEL-positive cells in cancer cell lines and normal lung fibroblast after 72 hours from radiation treatment. The cells were cultured before IR in control medium (CM) or short-term starvation medium (STS).

3.6. TUNEL apoptotic cell detection

Since previous results have indicated that IR inhibited cell growth, cell viability, and promote cell cycle arrest, we tested the effect of IR on cell death. To further explore the mechanism by which STS could enhance the radiation effect on cell lines, we investigated whether STS could promote IR-induced apoptosis.

Apoptotic cell death following exposure to irradiation was quantified after 72 hours using TUNEL assay by flow-cytometry **(Fig.6)**. As shown in **Figure 6A** IR in combination with moderate STS reduced the rate of TUNEL-positive cells of 3,7% in MRC5 cell line compared to IR alone. This data confirmed the previous observations regarding a protective role of STS in normal cell line. Instead, no difference in the percentage of apoptotic cells, between CM and STS pre-conditions, was observed in cancer cell lines, except for A549 where TUNEL-positive cells increased of 38.9 % in STS medium **(Fig.6B)**.

The data indicate that the metastatic cell lines are more sensitive to IR compared to adenocarcinoma cells **(Fig.6D-E)**.

3.7. Measure of DNA damage

Next, we hypothesized that STS condition may enhance IR sensitivity increasing the ability of irradiation to cause DNA damage. To test this hypothesis, we performed alkaline comet assay to determine the radio-responsiveness of normal and cancer cell lines in association with STS. The comet assay is the most popular test used to detect DNA damage at the level of a single cell.

We classified comets into five categories, from grade 0 to 4, according to % tail DNA value. The mean % tail DNA was chosen because it is directly proportional to DNA damage.

Categories were classified as follows: grade 0: 0 – 5, grade 1: ≥5 -15; grade 2: ≥25 -45; grade 3: ≥45 -70, grade 4: ≥70.

Other parameters, such as shape, tail length and olive tail moment are calculated to describe heterogeneity within cell population. The tail moment calculated by Olive et al (1990) defined as Olive tail moment, describes the variations in DNA distribution within tails. It is determined as the product of % tail DNA and tail moment length measured from the center of the head and the center of the tail of comet.

The basal level of DNA damage in non-irradiated cancer cells is ranging from 7.3% to 9.9%, while in normal cells is around 15%. As shown in **Fig 7** the amount of DNA damage in STS condition is

slightly increased in all cancer cells, conversely, we observed a reduction in DNA damage in normal cells.

The % tail DNA of irradiated fraction revealed a significant increase of at least 2-fold in DNA damage in starved-irradiated CFPAC1, and 0.25-fold in VCaP **(Fig 7B)**. In agreement with previous results, no statistically significant differences in the % tail DNA of the two irradiated fraction was observed in A549 cells, while a reduction in DNA damage was measured in A549sip53 in STS-irradiated fraction.
Remarkably, STS decrease the % tail DNA of MRC5 from 40% to 20%, suggesting a protective role of STS from IR damage.

All these data are confirmed by the major count of comet in class 0 and 1 in starved-irradiated cells, compared to treatment alone **(Fig.8A)**.

Instead, the STS in all tumor cell lines determined a minor number of comets in class 0 compared to control medium, while a major number of comets was counted in class 3 and 4 in irradiated cells than in the treatment alone **(Fig.8B-7E)**.

Taken together, these results strongly support previous observations whereby STS may increase radiation therapeutic index in metastatic cancer cell lines, and may protect normal cells from radiation damage.

Figure 7.

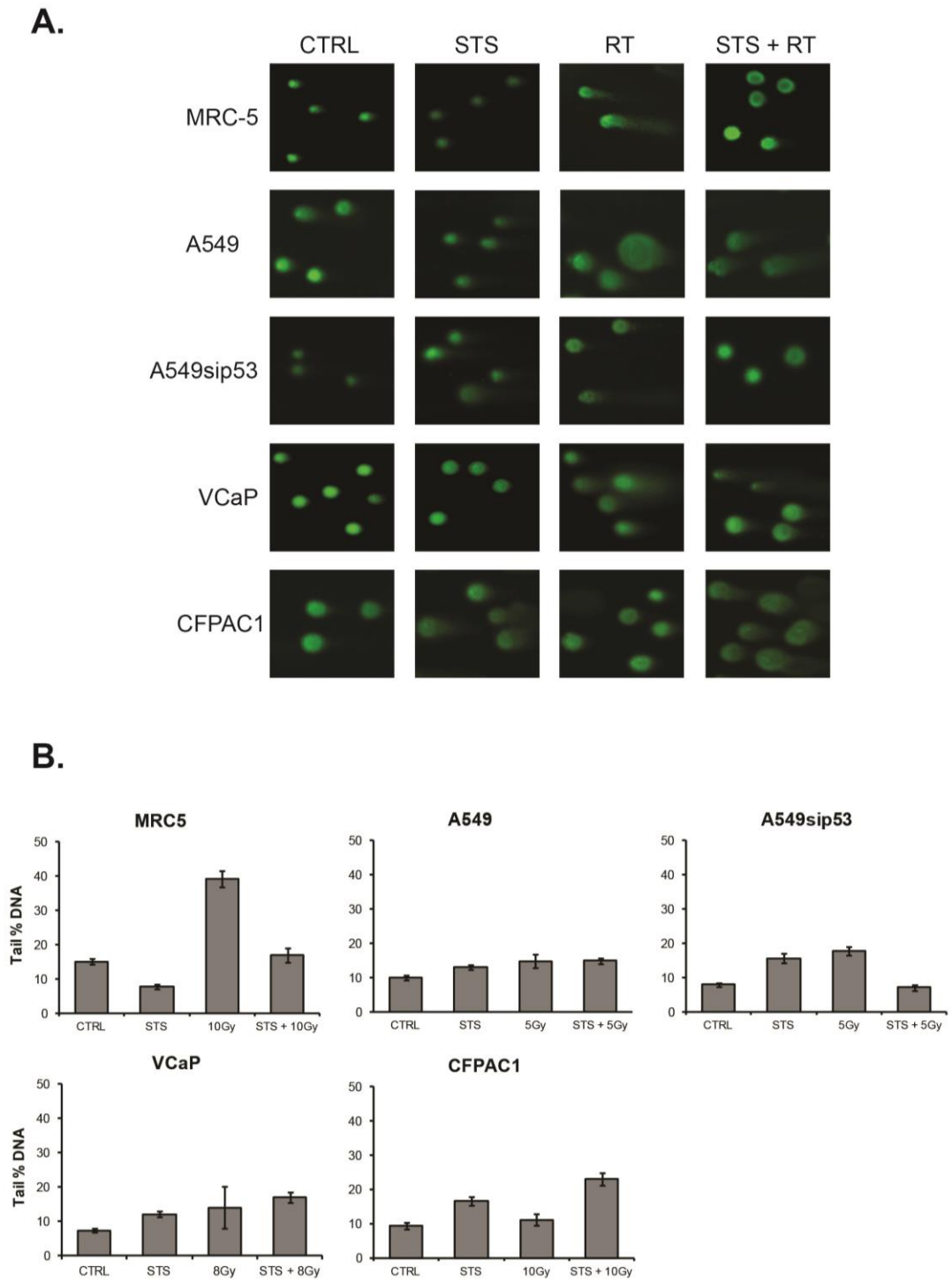

Figure 7: DNA damage measured by alkaline comet assay. A) Representative photomicrographs of comet assay showing cell lines stained with syber green after RT treatment and combination with STS, 10x magnification. B) DNA damage expressed as % tail DNA. Error bars represent mean ± SE. Statistical significance *p < 0.05, **p<0.01.

Figure 8.

A. **MRC5**

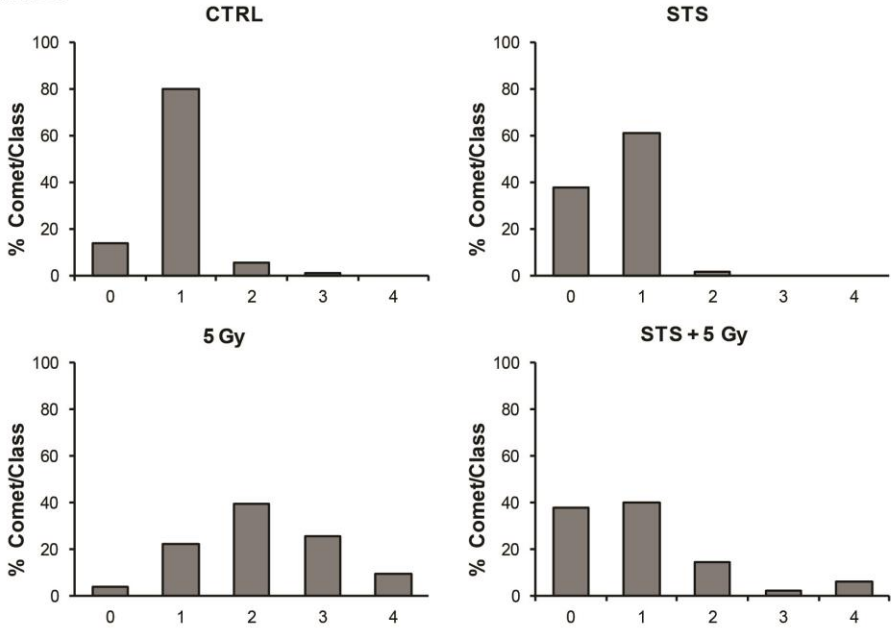

CTRL	Tail length (µm)	Tail Moment	Olive Tail Moment
Category	Mean ± SE	Mean ± SE	Mean ± SE
0	0,0 ± 0,0	0,0 ± 0,0	0,0 ± 0,0
1	20,8 ± 1,2	3,6 ± 0,3	4,2 ± 0,2
2	60,4 ± 16,6	22,1 ± 8,6	15,1 ± 4,1
3	121,0 ± 0,0	61,3 ± 0,0	33,0 ± 0,0
4	0,0 ± 0,0	0,0 ± 0,0	0,0 ± 0,0

5 Gy	Tail length (µm)	Tail Moment	Olive Tail Moment
Category	Mean ± SE	Mean ± SE	Mean ± SE
0	0,0 ± 0,0	0,0 ± 0,0	0,0 ± 0,0
1	26,1 ± 3,5	4,9 ± 1,0	4,9 ± 0,7
2	51,9 ± 4,2	18,9 ± 1,9	13,3 ± 1,0
3	104,6 ± 11,8	58,2 ± 7,4	33,4 ± 4,1
4	144,5 ± 17,9	115,3 ± 13,6	64,0 ± 12,3

STS	Tail length (µm)	Tail Moment	Olive Tail Moment
Category	Mean ± SE	Mean ± SE	Mean ± SE
0	0,3 ± 0,3	0,0 ± 0,0	0,0 ± 0,0
1	11,8 ± 0,5	1,5 ± 0,1	2,4 ± 0,1
2	35,0 ± 0,0	8,8 ± 0,0	9,1 ± 0,0
3	0,0 ± 0,0	0,0 ± 0,0	0,0 ± 0,0
4	0,0 ± 0,0	0,0 ± 0,0	0,0 ± 0,0

STS+ 5 Gy	Tail length (µm)	Tail Moment	Olive Tail Moment
Category	Mean ± SE	Mean ± SE	Mean ± SE
0	3,3 ± 0,6	0,1 ± 0,0	0,4 ± 0,1
1	17,9 ± 1,8	2,6 ± 0,4	3,6 ± 0,3
2	39,9 ± 3,6	13,2 ± 1,1	11,3 ± 0,9
3	89,0 ± 12,0	59,0 ± 9,5	41,3 ± 5,7
4	111,8 ± 9,5	93,6 ± 10,9	58,5 ± 5,5

B.

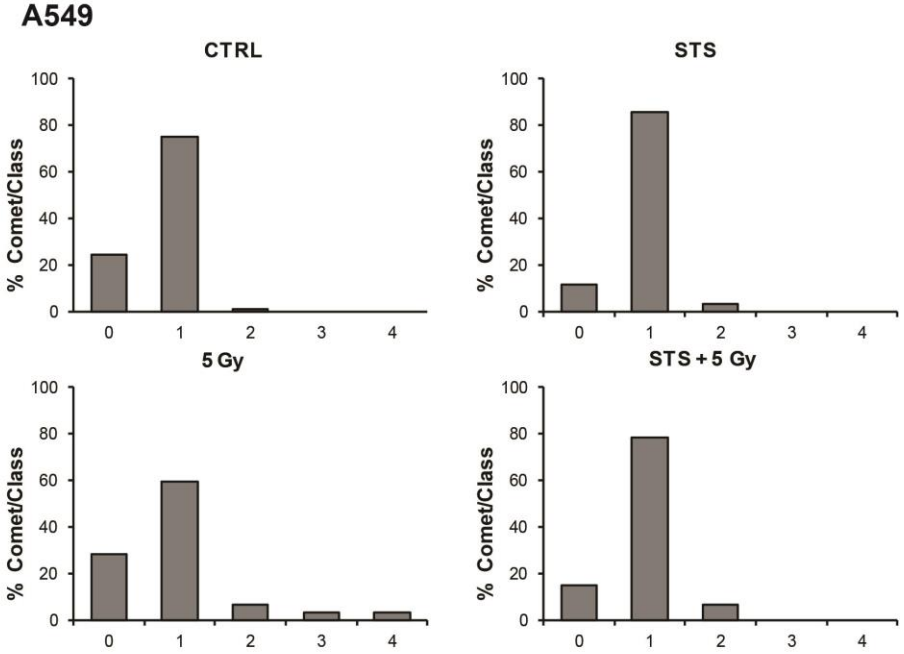

CTRL	Tail length (µm)	Tail Moment	Olive Tail Moment
Category	Mean ± SE	Mean ± SE	Mean ± SE
0	0,0 ± 0,0	0,0 ± 0,0	0,0 ± 0,0
1	17,2 ± 0,9	2,4 ± 0,2	3,3 ± 0,2
2	44,0 ± 0,0	16,1 ± 0,0	12,5 ± 0,0
3	0,0 ± 0,0	0,0 ± 0,0	0,0 ± 0,0
4	0,0 ± 0,0	0,0 ± 0,0	0,0 ± 0,0

5 Gy	Tail length (µm)	Tail Moment	Olive Tail Moment
Category	Mean ± SE	Mean ± SE	Mean ± SE
0	0,9 ± 0,4	0,0 ± 0,0	0,1 ± 0,1
1	12,7 ± 0,6	1,8 ± 0,2	2,6 ± 0,1
2	34,7 ± 12,5	11,8 ± 4,8	8,5 ± 2,1
3	129,0 ± 47,2	70,6 ± 25,7	43,0 ± 15,3
4	63,0 ± 1,0	63,0 ± 1,0	0,0 ± 0,0

STS	Tail length (µm)	Tail Moment	Olive Tail Moment
Category	Mean ± SE	Mean ± SE	Mean ± SE
0	0,0 ± 0,0	0,0 ± 0,0	0,0 ± 0,0
1	18,6 ± 0,8	2,8 ± 0,2	3,5 ± 0,2
2	51,7 ± 12,6	16,5 ± 5,9	13,8 ± 4,1
3	0,0 ± 0,0	0,0 ± 0,0	0,0 ± 0,0
4	0,0 ± 0,0	0,0 ± 0,0	0,0 ± 0,0

STS+ 5 Gy	Tail length (µm)	Tail Moment	Olive Tail Moment
Category	Mean ± SE	Mean ± SE	Mean ± SE
0	0,0 ± 0,0	0,0 ± 0,0	0,0 ± 0,0
1	28,8 ± 1,8	5,2 ± 0,4	5,4 ± 0,3
2	78,5 ± 25,9	23,5 ± 8,4	17,5 ± 6,2
3	0,0 ± 0,0	0,0 ± 0,0	0,0 ± 0,0
4	0,0 ± 0,0	0,0 ± 0,0	0,0 ± 0,0

C.

A549sip53

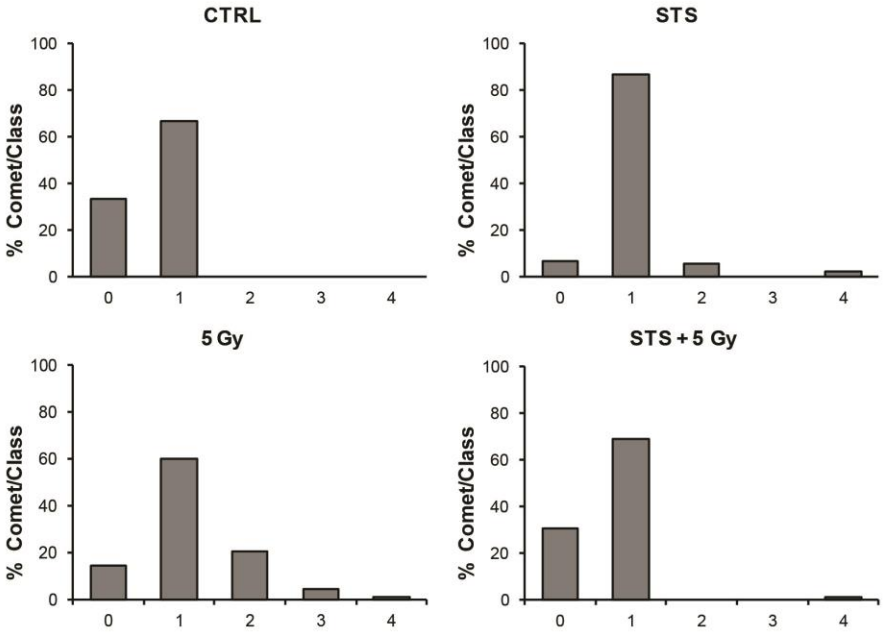

CTRL	Tail length (µm)	Tail Moment	Olive Tail Moment
Category	Mean ± SE	Mean ± SE	Mean ± SE
0	0,3 ± 0,2	0,0 ± 0,0	0,0 ± 0,0
1	11,5 ± 0,3	1,4 ± 0,1	2,4 ± 0,1
2	0,0 ± 0,0	0,0 ± 0,0	0,0 ± 0,0
3	0,0 ± 0,0	0,0 ± 0,0	0,0 ± 0,0
4	0,0 ± 0,0	0,0 ± 0,0	0,0 ± 0,0

5 Gy	Tail length (µm)	Tail Moment	Olive Tail Moment
Category	Mean ± SE	Mean ± SE	Mean ± SE
0	3,9 ± 1,0	0,2 ± 0,0	0,6 ± 0,1
1	21,2 ± 1,3	3,2 ± 0,3	4,0 ± 0,3
2	51,0 ± 6,1	16,8 ± 2,5	13,0 ± 1,6
3	141,2 ± 31,0	84,3 ± 20,8	52,6 ± 13,0
4	192,0 ± 0,0	142,2 ± 0,0	95,6 ± 0,0

STS	Tail length (µm)	Tail Moment	Olive Tail Moment
Category	Mean ± SE	Mean ± SE	Mean ± SE
0	0,0 ± 0,0	0,0 ± 0,0	0,0 ± 0,0
1	14,4 ± 0,5	2,2 ± 0,1	2,9 ± 0,1
2	37,0 ± 4,1	10,7 ± 2,0	9,0 ± 1,3
3	0,0 ± 0,0	0,0 ± 0,0	0,0 ± 0,0
4	72,5 ± 6,5	72,5 ± 6,5	0,0 ± 0,0

STS+ 5 Gy	Tail length (µm)	Tail Moment	Olive Tail Moment
Category	Mean ± SE	Mean ± SE	Mean ± SE
0	1,4 ± 0,4	0,1 ± 0,0	0,2 ± 0,1
1	8,5 ± 0,2	0,8 ± 0,0	1,5 ± 0,1
2	0,0 ± 0,0	0,0 ± 0,0	0,0 ± 0,0
3	0,0 ± 0,0	0,0 ± 0,0	0,0 ± 0,0
4	69,0 ± 0,0	69,0 ± 0,0	0,0 ± 0,0

D.

CFPAC1

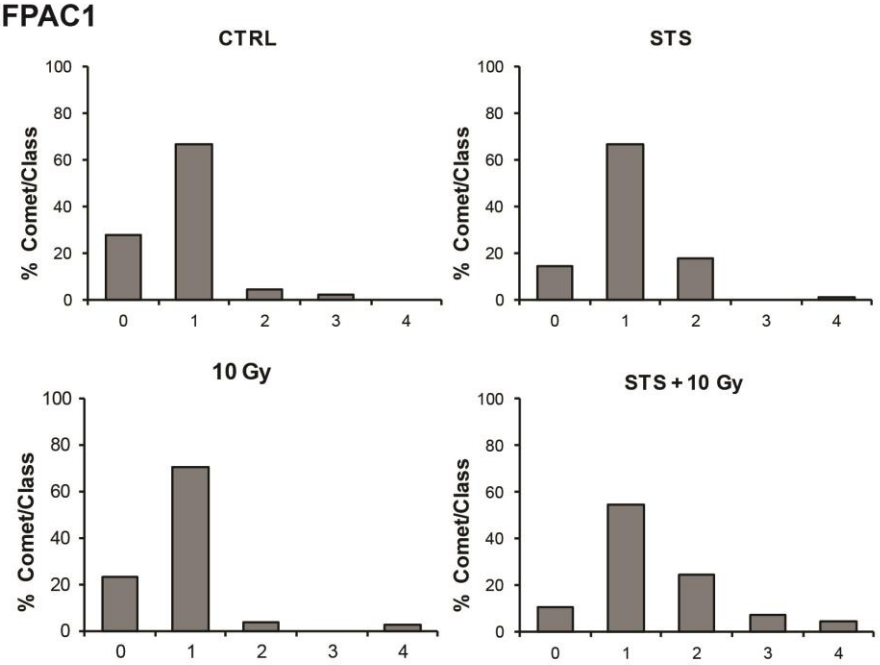

CTRL	Tail length (µm)	Tail Moment	Olive Tail Moment
Category	Mean ± SE	Mean ± SE	Mean ± SE
0	0,7 ± 0,5	0,0 ± 0,0	0,1 ± 0,1
1	28,6 ± 2,0	3,3 ± 0,4	4,2 ± 0,3
2	105,0 ± 20,6	36,6 ± 11,5	23,4 ± 5,2
3	174,5 ± 5,5	98,6 ± 0,2	8,3 ± 5,2
4	0,0 ± 0,0	0,0 ± 0,0	0,0 ± 0,0

STS	Tail length (µm)	Tail Moment	Olive Tail Moment
Category	Mean ± SE	Mean ± SE	Mean ± SE
0	1,2 ± 0,6	0,1 ± 0,0	0,2 ± 0,1
1	24,8 ± 1,8	4,2 ± 0,5	5,2 ± 0,4
2	46,8 ± 7,9	15,7 ± 3,2	13,2 ± 2,0
3	71,0 ± 0,0	38,7 ± 0,0	25,0 ± 0,0
4	81,0 ± 0,0	81,0 ± 0,0	0,0 ± 0,0

10 Gy	Tail length (µm)	Tail Moment	Olive Tail Moment
Category	Mean ± SE	Mean ± SE	Mean ± SE
0	4,5 ± 1,0	0,2 ± 0,0	0,6 ± 0,1
1	19,8 ± 1,5	2,4 ± 0,4	3,5 ± 0,3
2	76,5 ± 16,8	23,0 ± 3,8	15,7 ± 1,9
3	0,0 ± 0,0	0,0 ± 0,0	0,0 ± 0,0
4	75,0 ± 7,5	75,0 ± 7,5	0,0 ± 0,0

STS+ 10 Gy	Tail length (µm)	Tail Moment	Olive Tail Moment
Category	Mean ± SE	Mean ± SE	Mean ± SE
0	0,0 ± 0,0	0,0 ± 0,0	0,0 ± 0,0
1	22,3 ± 1,5	3,7 ± 0,4	4,7 ± 0,4
2	56,1 ± 3,3	18,7 ± 1,2	15,1 ± 0,7
3	90,8 ± 14,9	46,1 ± 7,9	29,5 ± 4,5
4	135,0 ± 22,1	113,5 ± 9,9	30,8 ± 20,0

E.

VCaP

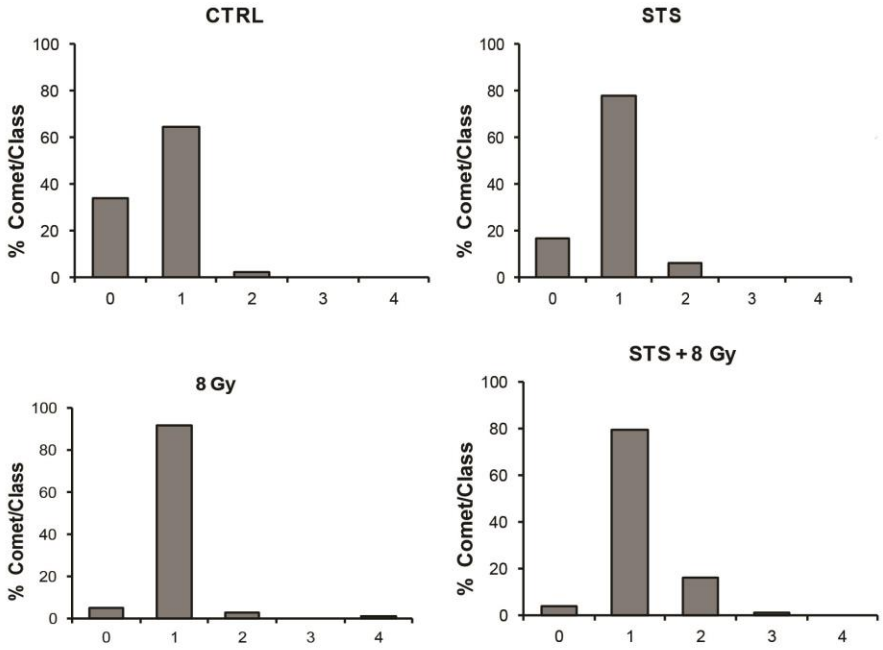

CTRL	Tail length (um)	Tail Moment	Olive Tail Moment
Category	Mean ± SE	Mean ± SE	Mean ± SE
0	0,5 ± 0,3	0,0 ± 0,0	0,1 ± 0,0
1	12,5 ± 0,6	1,5 ± 0,1	2,5 ± 0,2
2	31,0 ± 2,0	8,1 ± 0,8	8,1 ± 0,7
3	0,0 ± 0,0	0,0 ± 0,0	0,0 ± 0,0
4	0,0 ± 0,0	0,0 ± 0,0	0,0 ± 0,0

STS	Tail length (um)	Tail Moment	Olive Tail Moment
Category	Mean ± SE	Mean ± SE	Mean ± SE
0	0,0 ± 0,0	0,0 ± 0,0	0,0 ± 0,0
1	18,1 ± 0,9	2,7 ± 0,2	3,6 ± 0,2
2	40,5 ± 3,3	13,1 ± 1,6	11,1 ± 1,1
3	0,0 ± 0,0	0,0 ± 0,0	0,0 ± 0,0
4	0,0 ± 0,0	0,0 ± 0,0	0,0 ± 0,0

8 Gy	Tail length (um)	Tail Moment	Olive Tail Moment
Category	Mean ± SE	Mean ± SE	Mean ± SE
0	0,0 ± 0,0	0,0 ± 0,0	0,0 ± 0,0
1	20,0 ± 1,1	2,7 ± 0,3	3,8 ± 0,3
2	67,0 ± 23,0	17,9 ± 5,0	14,5 ± 2,8
3	0,0 ± 0,0	0,0 ± 0,0	0,0 ± 0,0
4	70,0 ± 0,0	70,0 ± 0,0	0,0 ± 0,0

STS+ 8 Gy	Tail length (um)	Tail Moment	Olive Tail Moment
Category	Mean ± SE	Mean ± SE	Mean ± SE
0	2,0 ± 2,0	0,1 ± 0,1	0,2 ± 0,2
1	30,6 ± 2,2	4,4 ± 0,5	5,4 ± 0,4
2	81,4 ± 9,3	24,8 ± 3,3	18,4 ± 2,3
3	202,0 ± 0,0	113,5 ± 0,0	64,2 ± 0,0
4	0,0 ± 0,0	0,0 ± 0,0	0,0 ± 0,0

Figure 8: Quantitative analysis of comet categories. The comet parameters, such as tail length, tail moment and olive tail moment are indicated in tables. The values represent the mean obtained from 100 comets ± SE.

Furthermore, we detected directly the DNA damage measuring phosphorylate histone H2AX foci (γ-H2AX) in the cell nuclei as indicator of cellular radiosensitivity **(Fig. 9A)**. γ-H2AX phosphorylation indicates the presence of double-strand DNA breaks and could serve as a biomarker for chemotherapy toxicity in healthy cells. The results showed γ-H2AX foci in metastatic cell lines CFPAC1 and VCaP when exposed to radiation. In particular, pre-incubation with STS medium 24 hours before radiotherapy resulted in 2-fold increase of γ-H2AX foci comparedto IR alone in CFPAC1. Instead this trend is not maintained in metastatic prostate cells.

In agreement with previous observations, we did not detect foci in adenocarcinoma cell lines and in normal cells underlining an absence of DNA damage.

Moreover, cells were stained withRad51, which accumulates at sites of broken DNA **(Fig. 9B)**. We next counted the number of Rad51 foci and observed a high quantitative of DNA damage in MRC5 cell line in normal condition, denoting a protecting role of STS. Like γ-H2AX detection, CFPAC1 exhibit DNA damage accumulation after irradiation with an increase of Rad51 positive cells in STS condition.

3.8. Short-term starvation and gene expression

To better understand the mechanism through which radiotherapy was more effective combined with short-term starvation than with control medium in metastatic cells, we hypothesized that the low glucose level could be responsible for the activation or inactivation of genes involved in DNA damage repair machine. Furthermore, we evaluated the expression of glucose transporter GLUT-1 that is the main actor of the uptake of glucose from the surrounding medium into the cell. As shown in **Figure 10 (A-E)** the GLUT-1 expression in the different cell lines did not change. Probably because of the restoration of normal glucose concentration after 72h from starvation.

To investigate the potential synergic role of STS in association with irradiation treatment, we analyzed mRNA expression of PARP-1 (repair of single-strand breaks SSBs) and BRCA-1 (components of homologous recombination HR repair system) genes. We observed after 72 hours a significant increase in BRCA-1 expression when radiotherapy is preceded by STS and a significant reduction of PARP-1 expression only in lung cancer cell lines. In conclusion, these results confirmed that the repair DNA genes are long activated in lung cancer cell lines maintained in low glucose conditions compared to the other cell lines, and that A549 are more sensitive compared to A549 sip53.

Figure 9.

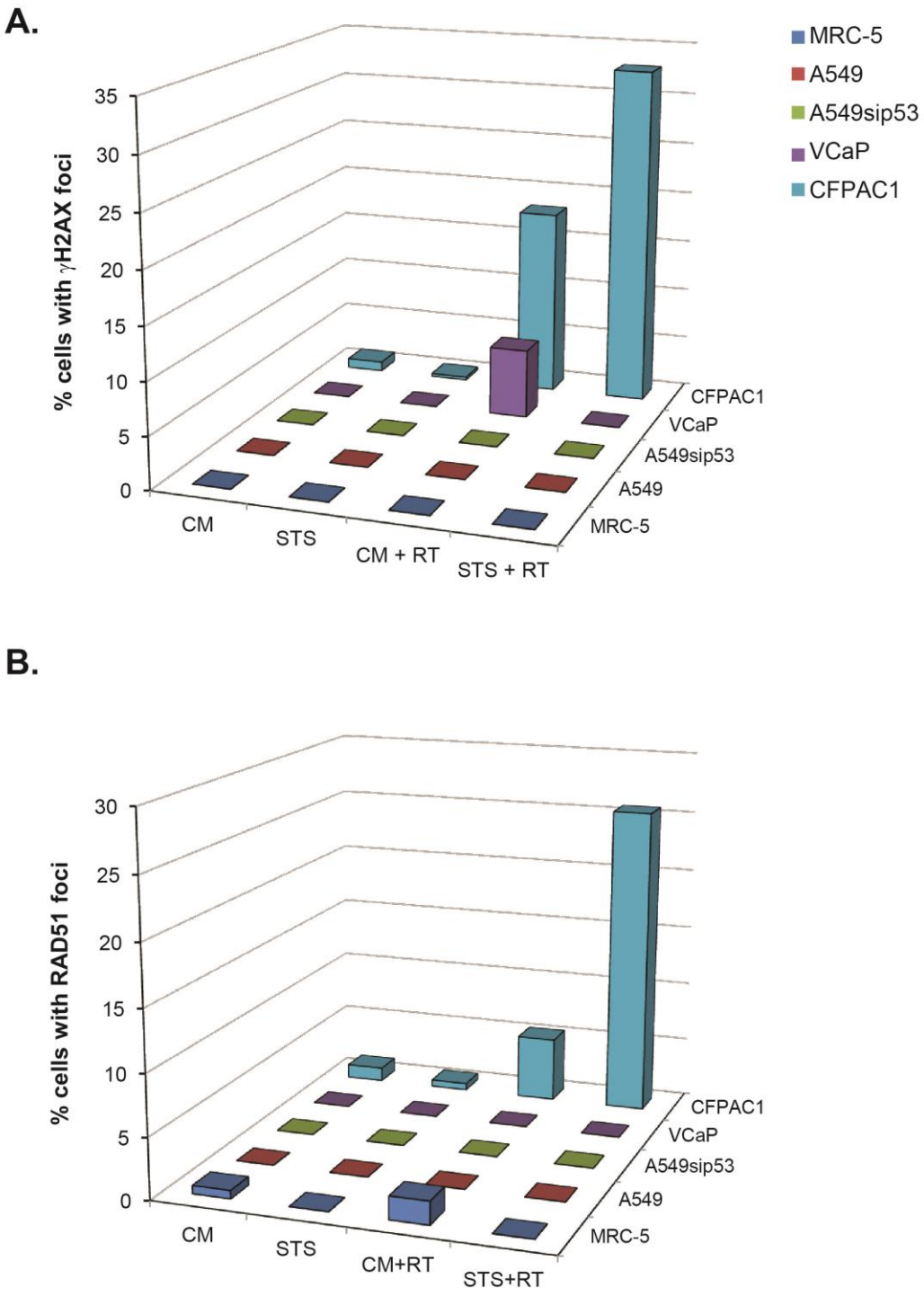

Figure 9: Imaging quantification of γH2AX and RAD51 foci. Cell lines were cultured on coverslips in control (CM) or short-term starvation medium (STS) for 24h, and then treated with IR and stained at 72h. At least 100 cells were scored for each condition. The percentage of positive cells for γH2AX-foci (A) and for RAD51-foci (B) was calculated. Cells with more than 5 foci were scored as positive.

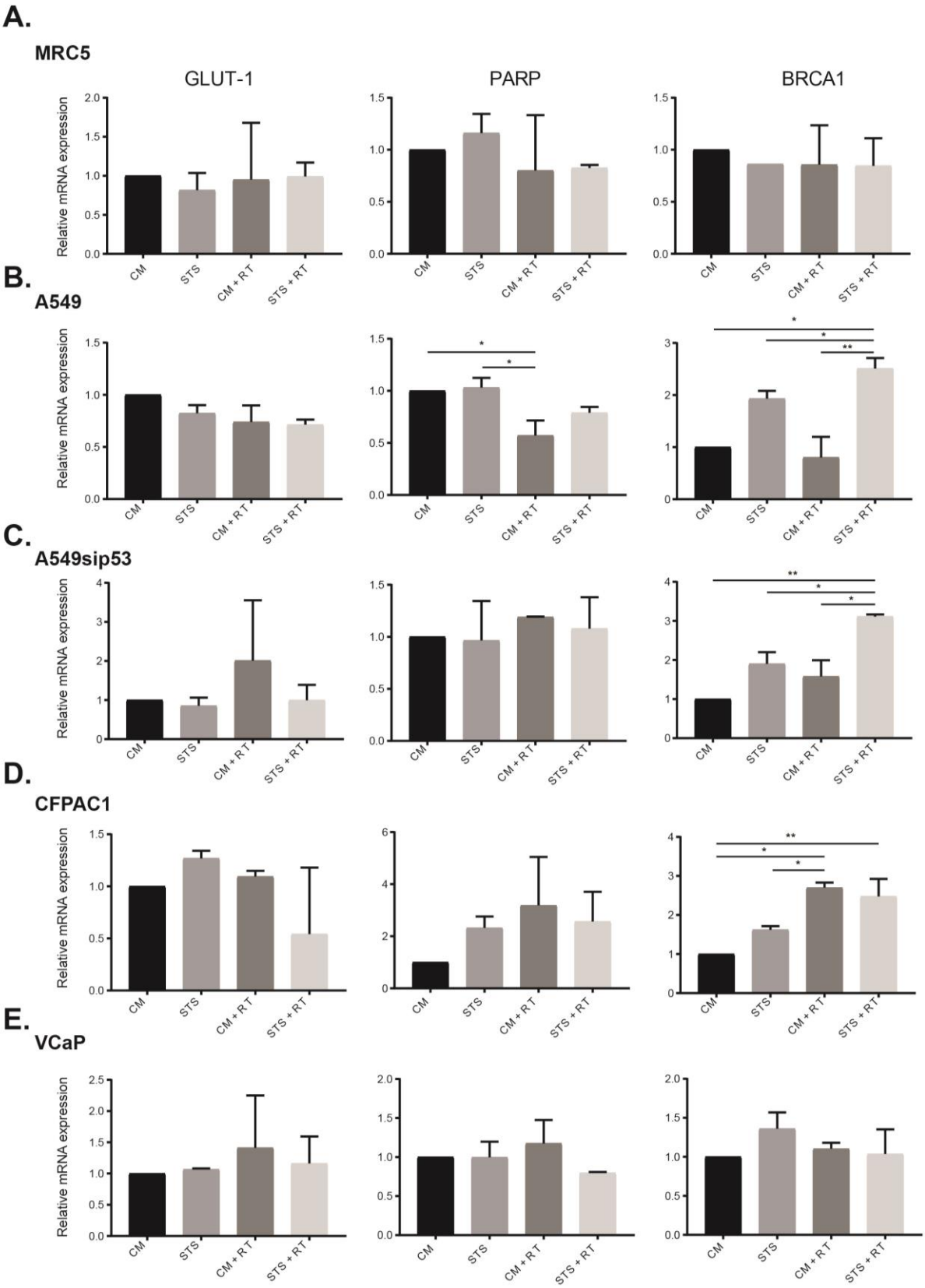

Figure 10: Effects of radiation on mRNA expression. mRNA was isolated after 72hours from irradiation treatment and gene expression was determined using quantitative real-time RT-PCR. Graphs are representative of two independent experiments, each performed in triplicate. Error bars represent SD of triplicate values. Statistical one-way ANOVA is used to test for differences groups. *$p < 0.05$, **$p<0.01$.

4. Discussion

Nowadays fasting, caloric restriction, fasting mimicking diet have become a popular topic in the field of oncology involving media, public opinion, marketing, and creating speculations and ambiguous messages. On the other hand, limited evidence in human studies have been shown how nutritional support improve the quality of life and survival in cancer patients (Caccialanza et al., 2018; O'Flanagan et al., 2017).

Recent studies *in vivo* and *in vitro* models demonstrated how short-term starvation or prolonged fasting (PF) could improve the efficacy of chemotherapy for some types of cancer with the possibility of protecting normal tissue against chemo-toxicity (Antunes et al., 2017; D'aronzo et al., 2015, Harvey et al., 2013; Huisman et al., 2015). At present few data are available on the effect of short-term starvation in association with radiotherapy (Simone et al., 2016). Thus, more preclinical studies are required to elucidate which kind of tumor, which stage, which therapy could effectively benefit from dietary approaches.

The aim of this study is to provide additional informations on radio-sensitizing starvation's effect in *in vitro* cancer cell lines and on protection in normal tissue.

To elucidate the biological mechanisms of activation and the effects induced by radiation during starvation, we used tumor cells from different tumor types and normal fibroblast as *in vitro* model. To better mimicking microenvironment *in vitro*, for each cell lines tested, we performed all the experiments in hypoxia condition. The oxygen partial pressure (pO_2) plays a fundamental role in the molecular and metabolic features of cells. Furthermore, as well know, Hif-1α,activated in hypoxia conditions, is one of the main transcription factor implicated in radiation resistance (Mckeown, 2014). On the basis of these observations, the meaningful role of microenvironment, both in normal and pathological issues, implies the tight control of *in vitro* experimental conditions to which the cells are exposed, in order to get as close as possible to the physiological conditions (Carreau et al., 2011).

In addition, in the present study, we used short-term starvation as a pre-condition to enhance radio-effect against cancer cells and to protect healthy cells.

Given that a starvation condition determines a differential cell cycle arrest, thus we hypothesized a protective G1/G2 selective cell cycle phase arrest and we explored the consequent potential vulnerabilities by nutrient deprivation of cancer cells to radiotherapy.

Our data show that short-term starvation of 24 hours perturbs cell cycle, determining almost a shift into G0/G1 cell cycle phase in normal fibroblasts associated with a strong reduction in S-phase and G2/M, while this phenomenon is less evident in cancer cells. The entry of almost all normal cells

into a high protection cell cycle arrest in response to short-term starvation, could reduce the damage of DNA induced by radiation.

In addition, we decided to evaluate the role of p53 in the induction of cell cycle arrest using a silenced p53 lung cancer cell line. We considered if protective effect of short-term starvation may be in part due to a regulation of cell cycle by p53, thus the presence of mutant p53 could be used as a strategy to not enter in a protective cell cycle status. Although our results show that the mutational status of p53, in adenocarcinoma model, is not responsible of a different response to radiotherapy by starved cell lines.

Here we report that metastatic cancer cells became more sensitive to radiotherapy in nutrient depletion medium, drastically reducing their colony forming growth, while normal cells were not affected. Instead, our preliminary results for adenocarcinoma cell lines, shown that in this kind of tumor the starvation does not improve the efficacy of radiotherapy also in a p53 mutational status independent manner.

As we expected, a short cell viability assay (72h) to test radiation treatment on the cell survival after different culture conditions, is not the best analysis setting. Notably, in this quick *in vitro* cell viability analysis, we observed a reduction of survival only in CFPAC1 cell line, the most sensitive cell line to radiotherapy. Instead, to better determine cell reproductive death after treatment with ionizing radiation, we used the gold standard clonogenic assay (Dunne et al., 2003). Our results demonstrate a reduction of the ability of single cell to grow into a colony in all metastatic cancer cell after radiation, with a complete inhibition when combined with 24 hours short-term starvation. Furthermore, the capacity to produce colonies is retained by normal fibroblast cells and is boosted when associated with starvation. As, previous data, in lung adenocarcinoma cells the radiation therapy is not reinforced by starvation, denoting a radio-sensitizing effect only in metastatic cell lines.

Previously published studies, indicate an increase in glucose consumption by tumor cells after irradiation (Dittmann et al., 2013). This high energy demand is required for DSB repair processes. In fact, tumor cells, which have a small intracellular amount of ATP, are dependent on glucose supply to induce chromatin relaxation by the radiation-induced histone H3- and H4-acetylation and consequently repair DNA DSBs. Instead, normal fibroblasts are characterized by high intracellular ATP levels that permit them to not be influenced by glucose starvation (Ampferl et al., 2018).

Recent studies demonstrate a role of nutrient deprivation in the regulation and activation of adaptive cellular response. We believed that short-term starvation may protect normal cells in part by

regulating cell cycle and influencing the activation of DNA repair machine. In support of our hypothesis we decided to measure DNA damage. Our comet assay experiments show an increase in DNA damage in starved-irradiated cancer cell lines, and a reduction in starved-irradiated normal cell, underlying a function of glucose deprivation in the regulation of repair pathways.

This could be one of the possible mechanism that explains why different starved-cells (normal and tumor) contribute in different ways to the response of DNA damage, however, further investigations are needed to better understand the metabolic changing and pathway regulation due to starvation.

Nutrient levels, such as glucose, could generate a protective environment that reduces DNA damage in healthy cells and at the same time create a hostile condition for tumor cells. Consistent with our results, other approaches (Mohanti et al., 1996; Singh et al., 1990) that used an analog of glucose to inhibit glycolytic pathway revealed an increase in radiation-induced damage.

GLUT1 is a member of glucose membrane transporters and its overexpression in cancer is frequently associated with chemo-resistance. Several studies demonstrated how the reduction of glucose and IGF-1, and the inhibition of mTOR pathway modulate the response to chemotherapy *in vitro* in cancer cells (Brandhorst et al., 2013; Sadfie et al., 2012). The glucose consumption is the preferred tumor metabolism, due to these reasons we expected that glucose transport is tightly regulated by glucose availability. Our results report that 24 hours of short-term starvation is not enough to down-regulate the GLUT1 expression for a long time as 72 hours, suggesting that the restoration of glucose could establish immediately the GLUT1 expression or that glucose-responsive elements are absent on GLUT1 (Klip et al., 1994).

Many metabolic changes due to radiation highlighting the need to understand how irradiation affects cancer cell response via changes in metabolism. PARP-1, a protein involved in the repair of single-strand breaks (SSBs), and BRCA1, an important component of the HR pathway, play an important role, not only in DNA repair pathways, but also in transcriptional regulation, cell death, angiogenesis, and metabolism (Bhute et al., 2016; Wu et al., 2010).

The metabolic alterations to oxidative phosphorylation or to glycolysis could result in a rapid ATP reduction, and a different regulation of PARP1 and BRCA1 proteins. Although our analysis of expression of some DNA damage pathways reveal a significant difference between lung adenocarcinoma cell lines, confirming the major resistance properties to irradition of A549sip53; and a high levels of BRCA1 in CFPAC1 cells after irradiation underlying the sensitiveness to radiotherapy.

Thus, the combination of radiation treatment with STS could improve radio-sensitivity in metastatic cancer cells, but not in normal fibroblast and in our *in vitro* model of lung carcinoma primary

tumor. Some studies show how, in order to adapt to a reduced oxygen environment (Hypoxia), cancer cells at the primary tumor site often undergo a metabolism reprogram from oxidative phosphorylation (OXPHOS) to glycolytic metabolism, while other metabolic strategies are activated by metastatic cells depending to colonization site. Such metabolic differences could influence the effect of glucose deprivation (Doppler et al., 2015).

In summary, the present study investigates whether short-term starvation before radiotherapy could be an effective approach with limited side-effects to improve the therapeutic efficacy of radiation therapy and to preserve healthy tissue. The aim of this study was to provide a scientific rationale for further preclinical and clinical studies, knowing that our *in vitro* investigations cannot directly be transferred into clinical practice without physiological, safety and feasibility parameters.

5. Conclusions

This study can provide potential powerful results about the simultaneous use of STS or fasting in combination with radiotherapy. This diet intervention could be a novel approach to improve the therapy efficacy, it may limit side effects and preserve healthy tissue. Furthermore, new radiation schemes, such as high single dose fraction in combination with STS, could represent an alternative treatment option for patients with metastatic tumors.

The data generated in this study could be used as radiobiological basis for further preclinical and clinical studies.

5. References

Ahrendt, S. A., Y. Hu, M. Buta, M. P. McDermott, N. Benoit, S. C. Yang, L. Wu and D. Sidransky (2003). "p53 mutations and survival in stage I non-small-cell lung cancer: results of a prospective study." J Natl Cancer Inst **95**(13): 961-970.

Ampferl, R., H. P. Rodemann, C. Mayer, T. T. A. Höfling and K. Dittmann (2018). "Glucose starvation impairs DNA repair in tumour cells selectively by blocking histone acetylation." Radiother Oncol **126**(3): 465-470.

Antunes, F., M. Corazzari, G. Pereira, G. M. Fimia, M. Piacentini and S. Smaili (2017). "Fasting boosts sensitivity of human skin melanoma to cisplatin-induced cell death." Biochem Biophys Res Commun **485**(1): 16-22.

Apontes, P., O. V. Leontieva, Z. N. Demidenko, F. Li and M. V. Blagosklonny (2011). "Exploring long-term protection of normal human fibroblasts and epithelial cells from chemotherapy in cell culture." Oncotarget **2**(3): 222-233.

Bauersfeld, S. P., C. S. Kessler, M. Wischnewsky, A. Jaensch, N. Steckhan, R. Stange, B. Kunz, B. Brückner, J. Sehouli and A. Michalsen (2018). "The effects of short-term fasting on quality of life and tolerance to chemotherapy in patients with breast and ovarian cancer: a randomized cross-over pilot study." BMC Cancer **18**(1): 476

Berg JM, Tymoczko JL, Stryer L. Biochemistry. 5th edition. New York: W H Freeman; 2002. Section 30.3, Food Intake and Starvation Induce Metabolic Changes.Available from: https://www.ncbi.nlm.nih.gov/books/NBK22414/

Bhute, V. J., Y. Ma, X. Bao and S. P. Palecek (2016). "The Poly (ADP-Ribose) Polymerase Inhibitor Veliparib and Radiation Cause Significant Cell Line Dependent Metabolic Changes in Breast Cancer Cells." Sci Rep **6**: 36061.

Bianchi, G., R. Martella, S. Ravera, C. Marini, S. Capitanio, A. Orengo, L. Emionite, C. Lavarello, A. Amaro, A. Petretto, U. Pfeffer, G. Sambuceti, V. Pistoia, L. Raffaghello and V. D. Longo (2015). "Fasting induces anti-Warburg effect that increases respiration but reduces ATP-synthesis to promote apoptosis in colon cancer models." Oncotarget **6**(14): 11806-11819.

Brandhorst, S., E. Harputlugil, J. R. Mitchell and V. D. Longo (2017). "Protective effects of short-term dietary restriction in surgical stress and chemotherapy." Ageing Res Rev **39**: 68-77.

Brandhorst, S., M. Wei, S. Hwang, T. E. Morgan and V. D. Longo (2013). "Short-term calorie and protein restriction provide partial protection from chemotoxicity but do not delay glioma progression." Exp Gerontol **48**(10): 1120-1128.

Branzei, D. and M. Foiani (2008). "Regulation of DNA repair throughout the cell cycle." Nat Rev Mol Cell Biol **9**(4): 297-308.

Brown, J. M. and A. C. Koong (2008). "High-dose single-fraction radiotherapy: exploiting a new biology?" Int J Radiat Oncol Biol Phys **71**(2): 324-325.

Buono, R. and V. D. Longo (2018). "Starvation, Stress Resistance, and Cancer." Trends Endocrinol Metab **29**(4): 271-280.

Caccialanza, R., E. Cereda, F. De Lorenzo, G. Farina, P. Pedrazzoli and A.-S.-F. W. Group (2018). "To fast, or not to fast before chemotherapy, that is the question." BMC Cancer **18**(1): 337.

Cahill, G. F. (2006). "Fuel metabolism in starvation." Annu Rev Nutr **26**: 1-22.

Carreau, A., El Hafny-Rahbl, B., Matejuk, A., Grillon, C., Kleda, C. (2011). "Why is the partial oxygen pressure of human tissue a crucial parameter? Small molecules and hypoxia". J Cell Mol Med **15**(6): 1239-1253

Chua, K. L. M., I. Sin, K. W. Fong, M. L. K. Chua and H. Onishi (2017). "Stereotactic body radiotherapy for early stage lung cancer-historical developments and future strategies." Chin Clin Oncol **6**(Suppl 2): S20.

Crane, C. H. (2016). "Hypofractionated ablative radiotherapy for locally advanced pancreatic cancer." J Radiat Res **57 Suppl 1**: i53-i57.

D'Aronzo, M., M. Vinciguerra, T. Mazza, C. Panebianco, C. Saracino, S. P. Pereira, P. Graziano and V. Pazienza (2015). "Fasting cycles potentiate the efficacy of gemcitabine treatment in in vitro and in vivo pancreatic cancer models." Oncotarget **6**(21): 18545-18557.

De Bari, B., L. Porta, R. Mazzola, F. Alongi, A. D. Wagner, M. Schäfer, J. Bourhis and M. Ozsahin (2016). "Hypofractionated radiotherapy in pancreatic cancer: Lessons from the past in the era of stereotactic body radiation therapy." Crit Rev Oncol Hematol **103**: 49-61.

de Groot, S., M. P. Vreeswijk, M. J. Welters, G. Gravesteijn, J. J. Boei, A. Jochems, D. Houtsma, H. Putter, J. J. van der Hoeven, J. W. Nortier, H. Pijl and J. R. Kroep (2015). "The effects of short-term fasting on tolerance to (neo) adjuvant chemotherapy in HER2-negative breast cancer patients: a randomized pilot study." BMC Cancer **15**: 652.

Di Biase, S., H. S. Shim, K. H. Kim, M. Vinciguerra, F. Rappa, M. Wei, S. Brandhorst, F. Cappello, H. Mirzaei, C. Lee and V. D. Longo (2017). "Fasting regulates EGR1 and protects from glucose- and dexamethasone-dependent sensitization to chemotherapy." PLoS Biol **15**(3): e2001951.

Dietlein, F., L. Thelen and H. C. Reinhardt (2014). "Cancer-specific defects in DNA repair pathways as targets for personalized therapeutic approaches." Trends Genet **30**(8): 326-339.

Dittmann K, Mayer C, Rodemann HP, Huber SM. (2013). "EGFR cooperates with glucose transporter SGLT1 to enable chromatin remodeling in response to ionizing radiation." Radiother Oncol 107:247–51.

Dorff, T. B., S. Groshen, A. Garcia, M. Shah, D. Tsao-Wei, H. Pham, C. W. Cheng, S. Brandhorst, P. Cohen, M. Wei, V. Longo and D. I. Quinn (2016). "Safety and feasibility of fasting in combination with platinum-based chemotherapy." BMC Cancer **16**: 360.

Dunne, A. L., M. E. Price, C. Mothersill, S. R. McKeown, T. Robson and D. G. Hirst (2003). "Relationship between clonogenic radiosensitivity, radiation-induced apoptosis and DNA damage/repair in human colon cancer cells." Br J Cancer **89**(12): 2277-2283.

Döppler, H. and P. Storz (2015). "Differences in Metabolic Programming Define the Site of Breast Cancer Cell Metastasis." Cell Metab **22**(4): 536-537.

Foster, D. A., P. Yellen, L. Xu and M. Saqcena (2010). "Regulation of G1 Cell Cycle Progression: Distinguishing the Restriction Point from a Nutrient-Sensing Cell Growth Checkpoint(s)." Genes Cancer **1**(11): 1124-1131.

Ganapathy, S., A. Muraleedharan, P. S. Sathidevi, P. Chand and R. P. Rajkumar (2016). "CometQ: An automated tool for the detection and quantification of DNA damage using comet assay image analysis." Comput Methods Programs Biomed **133**: 143-154.

González Ruiz de León, C., M. Ramírez Backhaus, M. Sobrón Bustamante, J. Casaña, L. Arribas and J. Rubio-Briones (2017). "Radiation therapy for oligorecurrence in prostate cancer. Preliminary results of our centre." Actas Urol Esp **41**(10): 646-651.

Gyori, B. M., G. Venkatachalam, P. S. Thiagarajan, D. Hsu and M. V. Clement (2014). "OpenComet: an automated tool for comet assay image analysis." Redox Biol **2**: 457-465.

Harvey, A. E., L. M. Lashinger, D. Hays, L. M. Harrison, K. Lewis, S. M. Fischer and S. D. Hursting (2014). "Calorie restriction decreases murine and human pancreatic tumor cell growth, nuclear factor-κB activation, and inflammation-related gene expression in an insulin-like growth factor-1-dependent manner." PLoS One **9**(5): e94151.

Huisman, S. A., W. Bijman-Lagcher, J. N. IJzermans, R. Smits and R. W. de Bruin (2015). "Fasting protects against the side effects of irinotecan but preserves its anti-tumor effect in Apc15lox mutant mice." Cell Cycle **14**(14): 2333-2339.

IHME's Global Burden of Disease (GBD) Institute for Health Metrics and Evaluation (IHME). GBD Compare. Seattle, WA: IHME, University of Washington, 2015. Available from http://vizhub.healthdata.org/gbd-compare.)

Ikeda, M., S. Okada, K. Tokuuye, H. Ueno and T. Okusaka (2001). "Prognostic factors in patients with locally advanced pancreatic carcinoma receiving chemoradiotherapy." Cancer **91**(3): 490-495.

Javle, M. and N. J. Curtin (2011). "The role of PARP in DNA repair and its therapeutic exploitation." Br J Cancer **105**(8): 1114-1122.

Jensen, T. L., M. K. Kiersgaard, D. B. Sørensen and L. F. Mikkelsen (2013). "Fasting of mice: a review." Lab Anim 47(4): 225-240.

Joiner, M. and A. Van Der Kogel (2009). "Basic clinical Radiobiology."

Kennedy, T. A. C., M. T. Corkum and A. V. Louie (2017). "Stereotactic radiotherapy in oligometastatic cancer." Chin Clin Oncol **6**(Suppl 2): S16.

Klement, R. J. (2018). "Fasting, Fats, and Physics: Combining Ketogenic and Radiation Therapy against Cancer." Complement Med Res 25(2): 102-113.

Klip, A., T. Tsakiridis, A. Marette and P. A. Ortiz (1994). "Regulation of expression of glucose transporters by glucose: a review of studies in vivo and in cell cultures." FASEB J **8**(1): 43-53.

Lee, C. and V. D. Longo (2011). "Fasting vs dietary restriction in cellular protection and cancer treatment: from model organisms to patients." Oncogene **30**(30): 3305-3316.

Lettieri-Barbato, D. and K. Aquilano (2018). "Pushing the Limits of Cancer Therapy: The Nutrient Game." Front Oncol **8**: 148.

Lignot, J. H., LeMaho, Y. "A history of modern researc into fasting, starvation, and inanition." Chapter 2

Longo, V. D. and M. P. Mattson (2014). "Fasting: molecular mechanisms and clinical applications." Cell Metab **19**(2): 181-192.

Maurya, K. D., Devasagayam, P. A. (2011). "Role of radioprotectors in the inhibition of DNA dmage and modulation of DNA repair after exposure to gamma-radiation."

McCloskey, P., B. Balduyck, P. E. Van Schil, C. Faivre-Finn and M. O'Brien (2013). "Radical treatment of non-small cell lung cancer during the last 5 years." Eur J Cancer **49**(7): 1555-1564.

McKeown, S. R. (2014). "Defining normoxia, physoxia and hypoxia in tumours-implications for treatment response." Br J Radiol **87**(1035): 20130676.

Moebus, S., L. Göres, C. Lösch and K. H. Jöckel (2011). "Impact of time since last caloric intake on blood glucose levels." Eur J Epidemiol **26**(9): 719-728.

Mohanti, B. K., G. K. Rath, N. Anantha, V. Kannan, B. S. Das, B. A. Chandramouli, A. K. Banerjee, S. Das, A. Jena, R. Ravichandran, U. P. Sahi, R. Kumar, N. Kapoor, V. K. Kalia, B. S. Dwarakanath and V. Jain (1996). "Improving cancer radiotherapy with 2-deoxy-D-glucose: phase I/II clinical trials on human cerebral gliomas." Int J Radiat Oncol Biol Phys **35**(1): 103-111.

Morales, J., L. Li, F. J. Fattah, Y. Dong, E. A. Bey, M. Patel, J. Gao and D. A. Boothman (2014). "Review of poly (ADP-ribose) polymerase (PARP) mechanisms of action and rationale for targeting in cancer and other diseases." Crit Rev Eukaryot Gene Expr **24**(1): 15-28.

Neoptolemos, J. P., J. Kleeff, P. Michl, E. Costello, W. Greenhalf and D. H. Palmer (2018). "Therapeutic developments in pancreatic cancer: current and future perspectives." Nat Rev Gastroenterol Hepatol **15**(6): 333-348.

O'Flanagan, C. H., L. A. Smith, S. B. McDonell and S. D. Hursting (2017). "When less may be more: calorie restriction and response to cancer therapy." BMC Med **15**(1): 106.

Olive, P. L., J. P. Banáth and R. E. Durand (1990). "Heterogeneity in radiation-induced DNA damage and repair in tumor and normal cells measured using the "comet" assay." Radiat Res 122(1): 86-94.

Otsu N., "A threshold selection method from gray-level histograms, IEEE transactions on systems, man, and cybernetics", **9**(1):62-66, 1979.

Ouyang, H., P. Wang, Z. Meng, Z. Chen, E. Yu, H. Jin, D. Z. Chang, Z. Liao, L. Cohen and L. Liu (2011). "Multimodality treatment of pancreatic cancer with liver metastases using chemotherapy, radiation therapy, and/or Chinese herbal medicine." Pancreas **40**(1): 120-125.

Piccinini, F. (2015). "AnaSP: a software suite for automatic image analysis of multicellular spheroids." Comput Methods Programs Biomed **119**(1): 43-52.

Piccinini, F., E. Lucarelli, A. Gherardi and A. Bevilacqua (2012). "Multi-image based method to correct vignetting effect in light microscopy images." J Microsc **248**(1): 6-22.

Pignatta, S., C. Arienti, W. Zoli, M. Di Donato, G. Castoria, E. Gabucci, V. Casadio, M. Falconi, U. De Giorgi, R. Silvestrini and A. Tesei (2014). "Prolonged exposure to (R)-bicalutamide generates a LNCaP subclone with alteration of mitochondrial genome." Mol Cell Endocrinol **382**(1): 314-324.

Raffaghello, L., C. Lee, F. M. Safdie, M. Wei, F. Madia, G. Bianchi and V. D. Longo (2008). "Starvation-dependent differential stress resistance protects normal but not cancer cells against high-dose chemotherapy." Proc Natl Acad Sci U S A **105**(24): 8215-8220.

Rao, N., Bhimani, A. D., Papastefan, S. T., Kheirhah, P., Arnone G. D., Mehta, A. I.(2017) "Prostate spinal metastasis: an update and reviw." Cancer Research Frontiers **3**(1):72-82

Safdie, F., S. Brandhorst, M. Wei, W. Wang, C. Lee, S. Hwang, P. S. Conti, T. C. Chen and V. D. Longo (2012). "Fasting enhances the response of glioma to chemo- and radiotherapy." PLoS One **7**(9): e44603.

Safdie, F. M., T. Dorff, D. Quinn, L. Fontana, M. Wei, C. Lee, P. Cohen and V. D. Longo (2009). "Fasting and cancer treatment in humans: A case series report." Aging (Albany NY) **1**(12): 988-1007.

Scorsetti, M., M. Bignardi, F. Alongi, A. Fogliata, P. Mancosu, P. Navarria, S. Castiglioni, S. Pentimalli, A. Tozzi and L. Cozzi (2011). "Stereotactic body radiation therapy for abdominal targets using volumetric intensity modulated arc therapy with RapidArc: feasibility and clinical preliminary results." Acta Oncol **50**(4): 528-538.

Scott, S. L., P. H. Gumerlock, L. Beckett, Y. Li and Z. Goldberg (2004). "Survival and cell cycle kinetics of human prostate cancer cell lines after single- and multifraction exposures to ionizing radiation." Int J Radiat Oncol Biol Phys **59**(1): 219-227.

Shi, Y., E. Felley-Bosco, T. M. Marti, K. Orlowski, M. Pruschy and R. A. Stahel (2012). "Starvation-induced activation of ATM/Chk2/p53 signaling sensitizes cancer cells to cisplatin." BMC Cancer **12**: 571.

Simone, B. A., T. Dan, A. Palagani, L. Jin, S. Y. Han, C. Wright, J. E. Savage, R. Gitman, M. K. Lim, J. Palazzo, M. P. Mehta and N. L. Simone (2016). "Caloric restriction coupled with radiation decreases metastatic burden in triple negative breast cancer." Cell Cycle **15**(17): 2265-2274.

Singh, S. P., S. Singh and V. Jain (1990). "Effects of 5-bromo-2-deoxyuridine and 2-deoxy-D-glucose on radiation-induced micronuclei in mouse bone marrow." Int J Radiat Biol **58**(5): 791-797.

Slotman, B. J., K. H. Njo, A. de Jonge, O. W. Meijer and A. B. Karim (1993). "Hypofractionated radiation therapy in unresectable stage III non-small cell lung cancer." Cancer **72**(6): 1885-1893.
Taguchi, A., O. Delgado, M. Celiktaş, H. Katayama, H. Wang, A. F. Gazdar and S. M. Hanash (2014). "Proteomic signatures associated with p53 mutational status in lung adenocarcinoma." Proteomics **14**(23-24): 2750-2759.

Tekatli, H., N. Haasbeek, M. Dahele, P. De Haan, W. Verbakel, E. Bongers, S. Hashemi, E. Nossent, F. Spoelstra, A. J. de Langen, B. Slotman and S. Senan (2016). "Outcomes of

Hypofractionated High-Dose Radiotherapy in Poor-Risk Patients with "Ultracentral" Non-Small Cell Lung Cancer." J Thorac Oncol **11**(7): 1081-1089.

Tesei, A., A. Sarnelli, C. Arienti, E. Menghi, L. Medri, E. Gabucci, S. Pignatta, M. Falconi, R. Silvestrini, W. Zoli, V. D'Errico, A. Romeo, E. Parisi and R. Polico (2013). "In vitro irradiation system for radiobiological experiments." Radiat Oncol **8**: 257.

Tseng, C. L., W. Eppinga, R. Charest-Morin, H. Soliman, S. Myrehaug, P. J. Maralani, M. Campbell, Y. K. Lee, C. Fisher, M. G. Fehlings, E. L. Chang, S. S. Lo and A. Sahgal (2017). "Spine Stereotactic Body Radiotherapy: Indications, Outcomes, and Points of Caution." Global Spine J **7**(2): 179-197.

Warburg O, Posener K, Negelein E. Über den Stoffwechsel der Carcinomzelle. Biochem Zeitschr. 1924;152:309–44.

Withers, H. R. (1999). "Radiation biology and treatment options in radiation oncology." Cancer Res **59**(7 Suppl): 1676s-1684s.

World Cancer Research Fund / American Institute for Cancer Research. Food, Nutrition, Physical Activity, and the Prevention of Cancer: a Global Perspective. Washington, DC: AICR; 2007.

Wu, J., L. Y. Lu and X. Yu (2010). "The role of BRCA1 in DNA damage response." Protein Cell **1**(2): 117-123.

Yamada, H., S. Hirano, E. Tanaka, T. Shichinohe and S. Kondo (2006). "Surgical treatment of liver metastases from pancreatic cancer." HPB (Oxford) **8**(2): 85-88.

Zanoni, M., F. Piccinini, C. Arienti, A. Zamagni, S. Santi, R. Polico, A. Bevilacqua and A. Tesei (2016). "3D tumor spheroid models for in vitro therapeutic screening: a systematic approach to enhance the biological relevance of data obtained." Sci Rep **6**: 19103.